TECHNICAL REPORT STANDARD TITLE PAGE

1. Report No.	2. Government Accession No.	3. Recipient's Catalog No.
TX-97 3903-2		

4. Title and Subtitle	5. Report Date
Feasibility Study on Improvements to Dynamic Cone Penetrometer	April 1998
	6. Performing Organization Code

7. Author(s)	8. Performing Organization Report No.
S. Nazarian, V. Tandon, K. Crain and D. Yuan	Research Report 3903-2

9. Performing Organization Name and Address	10. Work Unit No.
Center for Highway Materials Research. The University of Texas at El Paso El Paso, Texas 79968-0516	11. Contract or Grant No. Study No. 7-3903

12. Sponsoring Agency Name and Address	13. Type of Report and Period Covered
Texas Department of Transportation P.O. Box 5051 Austin, Texas 78763	Report Sept. 1, 1996 -Aug 31, 1997
	14. Sponsoring Agency Code

15. Supplementary Notes

Research Performed in Cooperation with TxDOT
Research Study Title: Determining In-Place Engineering Properties of Lime or Cement Stabilized Pavement Layers

16. Abstract

One of the tools that its use in pavement engineering is becoming more common is the Dynamic Cone Penetrometer (DCP). In that test, a cone is penetrated into the ground under repeated impact loading. The rate of penetration as a function of depth is an indirect measurement of the strength of a layer. This test can reasonably quantify the layer thickness and qualify the type of material used. However, it is desirable to determine more quantitative information about the base and subgrade.

Two approaches were followed for this purpose. First, a DCP type device was constructed which contained a three dimensional accelerometer package in its tip. With this device, the modulus and Poisson's ratio of the base and subgrade can be determined with a minimal coring requirement. Second, an ordinary DCP was instrumented with a load cell and an accelerometer to determine the amount of energy imparted to the ground, and to determine the resistance to and amount of penetration of the device into the base and subgrade. This goal is achieved by theoretically simulating the penetration of a rod into a elastic medium.

The two devices were used at seven pavement sections to determine their versatility and field-worthiness. Both devices are proven to be feasible. However further work is needed to make them rugged, and more advanced analysis procedure is needed to more reliably extract data from them.

17. Key Words	18. Distribution Statement
Pavement Design, Modulus, Field Testing, Dynamic Cone Penetrometer, Seismic	No restrictions. This document is available to the public through the National Technical Information Service, 5285 Port Royal Road, Springfield, Virginia 22161

19. Security Classif. (of this report)	20. Security Classif. (of this page)	21. No. of Pages	22. Price
Unclassified	Unclassified	52	

Feasibility Study on Improvements to Dynamic Cone Penetrometer

by

Soheil Nazarian, Ph.D., P.E.
Vivek Tandon, Ph.D.
Kevin Crain, M.S.
and
Deren Yuan, Ph.D.

Research Project 7-3903

Determining In-Place Engineering Properties of Lime or Cement Stabilized Pavement Layers

Conducted for

Texas Department of Transportation

The Center for Highway Materials Research
The University of Texas at El Paso
El Paso, TX 79968-0516
Research Report 3903-2
April 1998

The contents of this report reflect the view of the authors, who are responsible for the facts and the accuracy of the data presented herein. The contents do not necessarily reflect the official views or policies of the Texas Department of Transportation. This report does not constitute a standard, specification, or regulation.

NOT INTENDED FOR CONSTRUCTION, BIDDING, OR PERMIT PURPOSES

Soheil Nazarian, Ph.D., P.E. (69263)
Vivek Tandon, Ph.D.
Kevin Crain, M.S.
Deren Yuan, Ph.D.

Acknowledgments

The authors would like to give their sincere appreciation to Elias Rmeili and Karl Nelson of TxDOTfor their support of this project.

We would also like to thank Dares Charoenphol and Raymond Guerra for their assistance in data reduction.

This was a colaborative project between UTEP and Texas Transportation Institute. The assistance provided by our conterparts from TTI is appreciated.

Abstract

One of the tools that its use in pavement engineering is becoming more common is the Dynamic Cone Penetrometer(DCP). While testing, a cone is penetrated into the ground under repeated impact loading. The rate of penetration (number of blows per mm) as a function of depth is an indirect measurement of the strength of a layer. This test can reasonably quantify the layer thickness and qualify the type of material used. However, it is desirable to determine more quantitative information about the base and subgrade.

Two approaches were followed for this purpose. First, a DCP type device was constructed which contained a three dimensional accelerometer package in its tip. With this device, the modulus and Poisson's ratio of the base and subgrade can be determined with a minimal coring requirement.

Second, an ordinary DCP was instrumented with a load cell and an accelerometer to determine the amount of energy imparted to the ground, and to determine the resistance to penetration of the device into the base and subgrade. This goal is achieved by theoretically simulating the penetration of a rod into a elastic medium.

The two devices were used at seven pavement sections in Bryan District in July 1997 to determine their versatility and field-worthiness. Both devices are proven to be feasible. However further work is needed to make them rugged, and more advanced analysis procedure is needed to extract data from them reliably.

Implementation Statement

The two devices are ready for limited implementation. Both devices seem to provide reasonable results. However, better interpretation software should be developed for them. Both devices should also be ruggedized for better field implementation.

The seimic DCP is the only device that can conveniently provide information about the Poisson's ratio of subgrade. The development of this device will be further pursued under Project 1735. The instrumnted DCP requires further field test to determine if the relationships developed are applicable to other districts of TxDOT.

We recommend that the devices be considered for further development. Also we recommend that they should be considered (on a trial basis) on some of the forensic projects and in conditions where other site investigation will be carried out.

Table of Contents

List of Tables

List of Figures

Feasibility Study on Improvements to Dynamic Cone Penetrometer

Introduction

One of the tools that its use in pavement engineering is becoming more common is the Dynamic Cone Penetrometer (DCP). During that test, a cone is penetrated into the ground under repeated impact loading. The rate of penetration (number of blows per mm) as a function of depth is an indirect measurement of the strength of a layer. This test can reasonably quantify the layer thickness and qualify the type of material used. However, it is desirable to determine more quantitative information about the base and subgrade.

Two approaches were followed for this purpose. First, a DCP type device was constructed which contained a three-dimensional accelerometer package in its tip. With this device, the modulus and Poisson's ratio of the base and subgrade can be determined with a minimal coring requirement.

Second, an ordinary DCP was instrumented with a load cell and an accelerometer to determine the amount of energy imparted to the ground, and to determine the resistance to penetration of the device into the base and subgrade. This goal is achieved by numerically simulating the penetration of a rod into an elastic medium.

The two devices were used at seven pavement sections in Bryan District in July 1997 to determine their versatility and field-worthiness. Both devices are proven to be feasible. However further work is needed to make them rugged, and more advanced analysis procedure is required to extract data from them more reliably.

The Seismic Pavement Analyzer (SPA) was also used at these sites. The relationships among the results from these devices and other nondestructive testing (NDT) devices such as the Falling Weight Deflectometer (FWD), the Dynaflect, and the Ground Penetrating Radar (GPR) used at these sites are also of interest. This report contains the results from the seismic and instrumented DCPs and the SPA. In the near future a report that comprehensively compares the results from field data at seven sites in Bryan District will be submitted to TxDOT in conjunction with our collaborators at TTI.

Dynamic Cone Penetrometer (DCP)

A dynamic cone penetrometer, as shown in Figure 1, consists of a steel rod with a cone at one end and an anvil on the other. The rod is driven into the base or subgrade by dropping a hammer with a mass of 4.5 to 8 kg on top of the anvil from a height of about 565 mm.

While testing, the number of blows and the depth of penetration are recorded. The outcome of interest from the DCP is the penetration resistance in blows per mm. Typical results from one site are shown in Figure 2. Based on extensive work in South Africa (such as Kleyn and Savage, 1982), the US (such as Webster et al., 1992) and Israel (such as Ninveh and Ishai, 1985), correlations between the DCP penetration resistance and the CBR values have been made. One such example is shown in Figure 3. As shown in the figure, developing a universal relationship between the DCP and the CBR may be difficult. However, for each soil unit in a certain area such relationship should be developed.

The DCP device is becoming more popular because of its ease of use and low cost. However, one of the concerns with the method is that the results are qualitative rather than representing an engineering property. By instrumenting the device, more quantitative information can be retrieved.

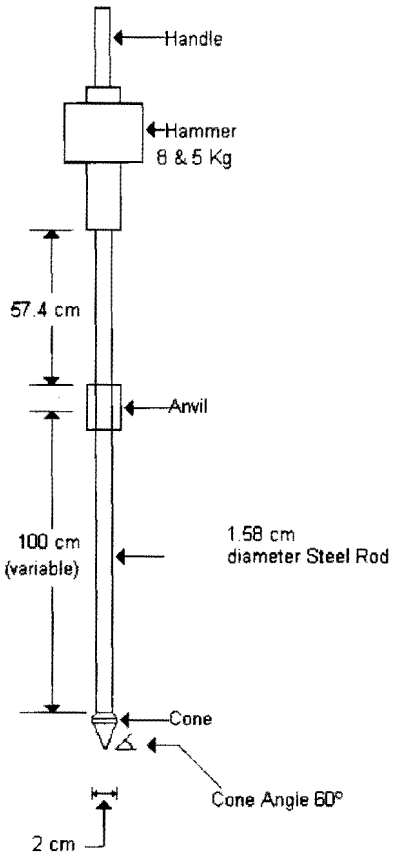

Figure 1 - A Typical Dynamic Cone Penetration (DCP) Device (from Webster et al, 1992)

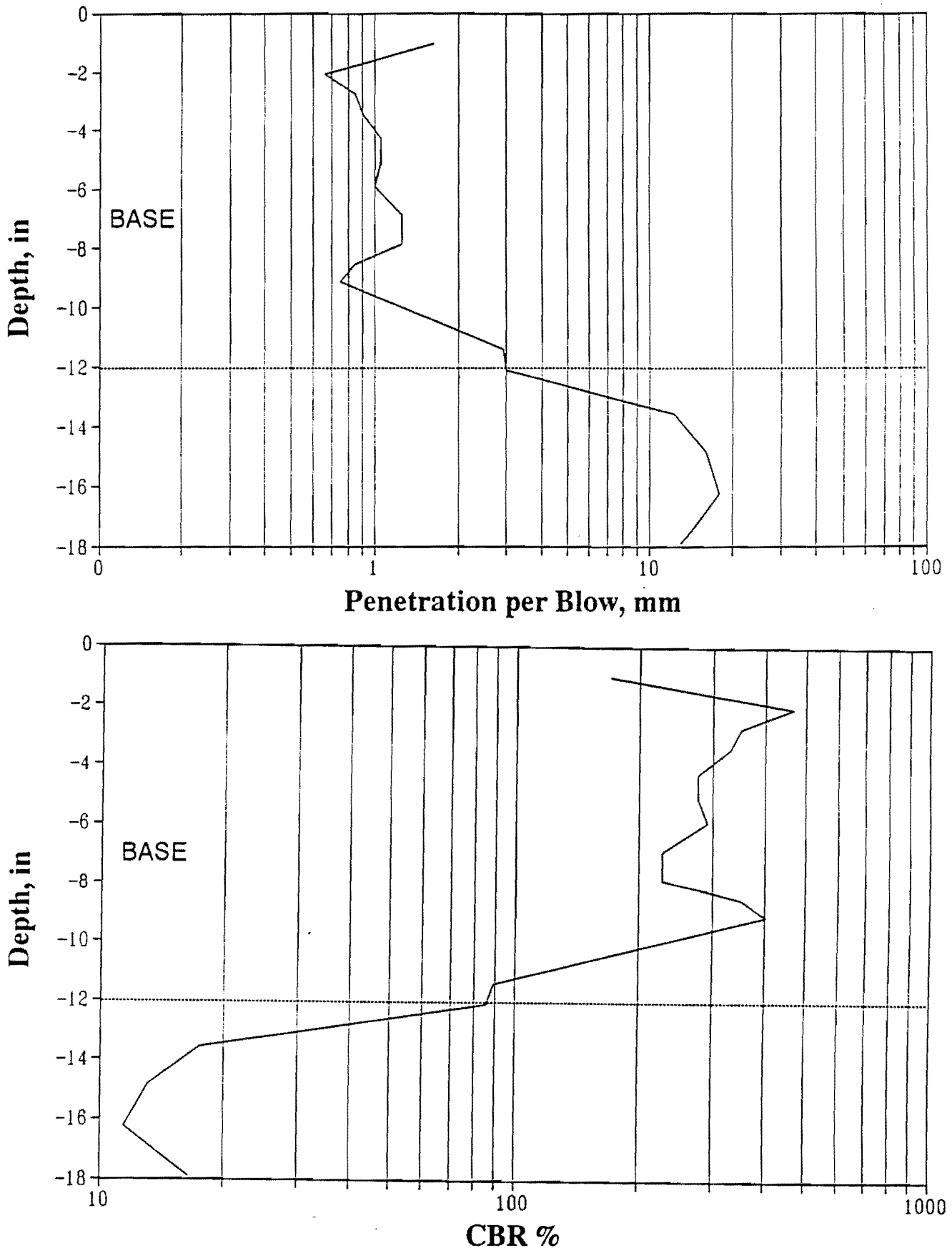

Figure 2 - Typical Results from a DCP Device

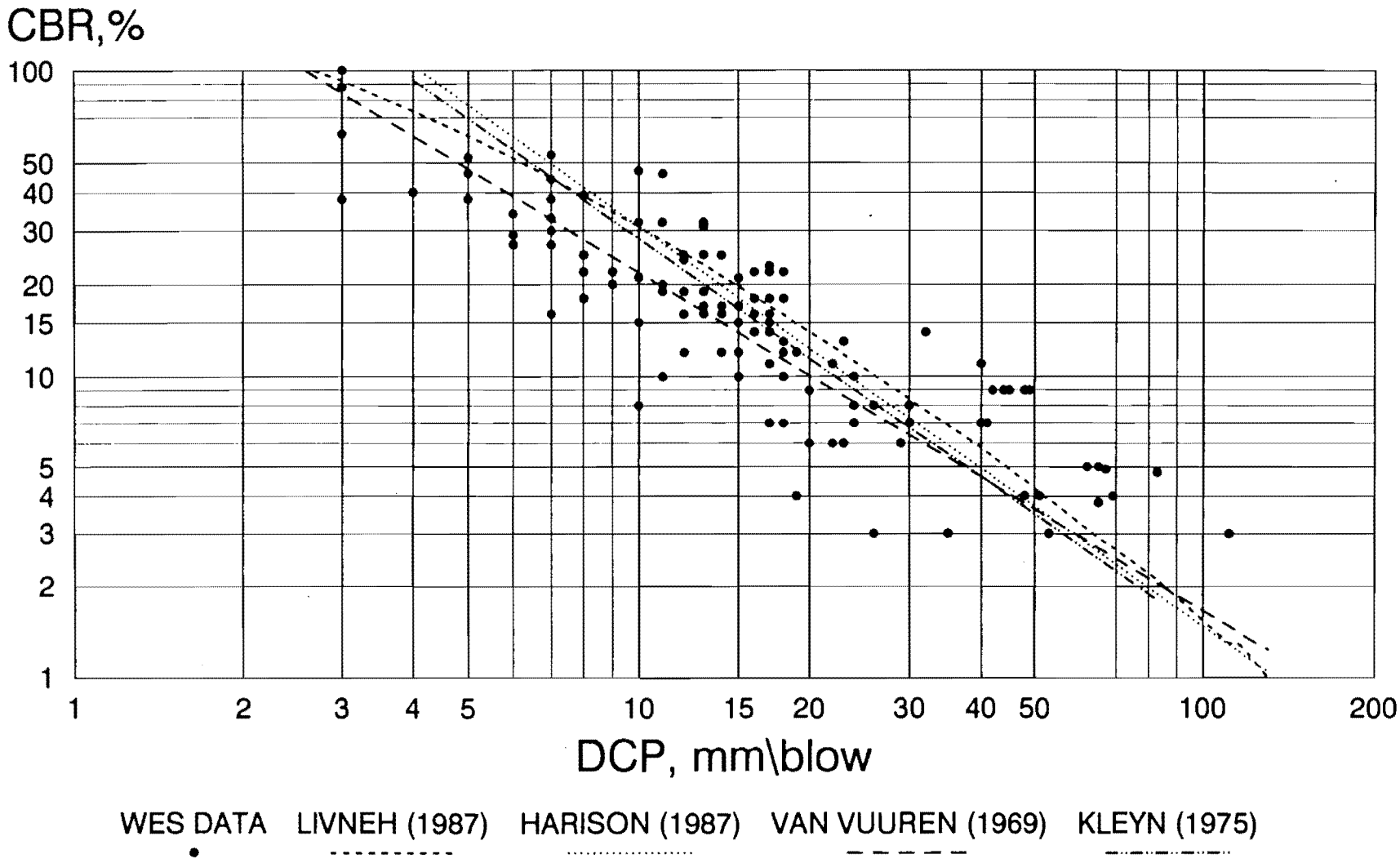

Figure 3 - Typical Correlation between CBR and DCP Penetration Resistance (from Webster et al., 1992)

Seismic Dynamic Cone Penetrometer (SDCP)

The SDCP consists of a rod similar to that of the DCP with a tip similar to that of the DCP. However, a three-dimensional accelerometer package has been retrofitted in the tip (see Figure 4). The modulus and Poisson's ratio of the base and subgrade can be measured with the added sensors as described below. Shinn et al. (1988) have developed a similar device but for deep geotechnical strata.

The test procedure is very similar to the so-called downhole seismic test (Woods, 1991). The schematic of downhole seismic tests is shown in Figure 5. The equipment needed to perform this test, besides the SDCP, are an ordinary 500-gr hammer, an oscilloscope, and a trigger mechanism. The trigger mechanism consists of an R-C circuit. The hammer and a small conductive metal object, are connected to the circuitry. When the hammer impacts the metal object, the capacitor of the R-C circuit discharges the voltage quite rapidly. The energy discharge is monitored by the oscilloscope, so that the time of impact ("time zero") can be determined. Upon the activation of the trigger the responses of these accelerometers are also recorded so that the travel times of different types of waves can be determined.

To perform a test, the tip of the SDCP is placed at a given depth. The pavement surface is then impacted with a small hand-held hammer. The records from the receivers are retrieved and saved for future analysis. The reduction of data consists of determining the arrivals of different waves.

Motion created by the hammer can be described by two kinds of waves: compression waves and shear waves. Collectively, these waves are called body waves, as they travel within the body of the medium. Compression and shear waves can be distinguished by the direction of particle motion relative to the direction of wave propagation.

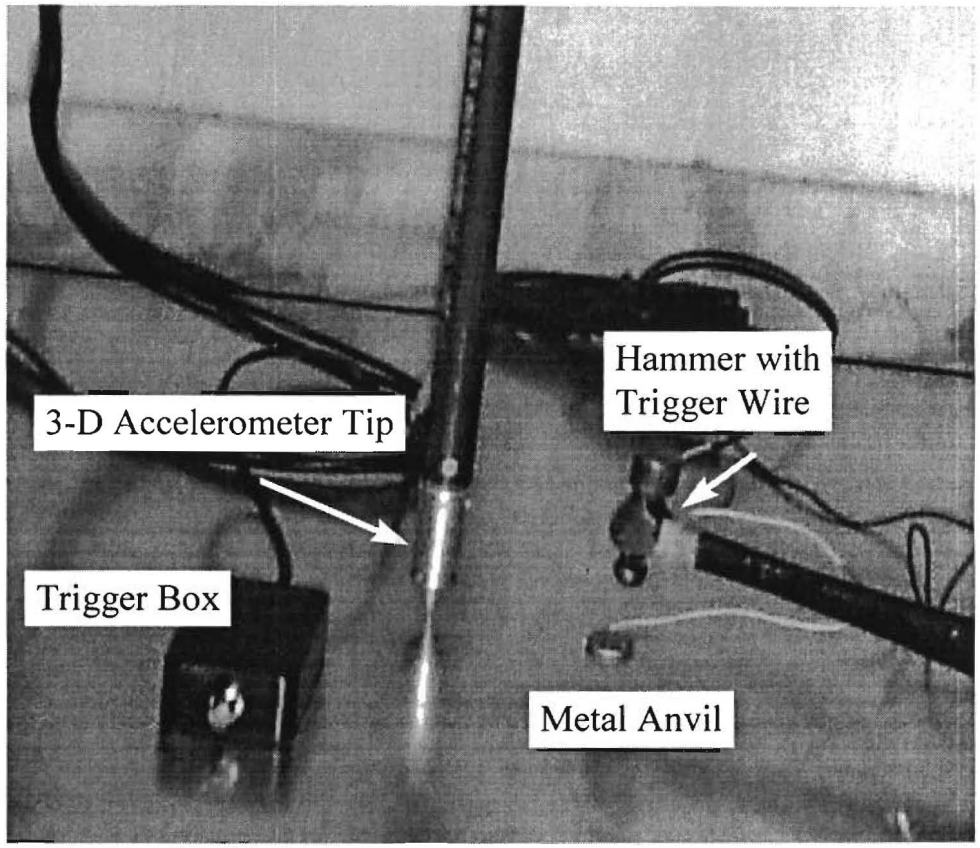

Figure 4 - Seismic Dynamic Cone Penetration (SDCP)

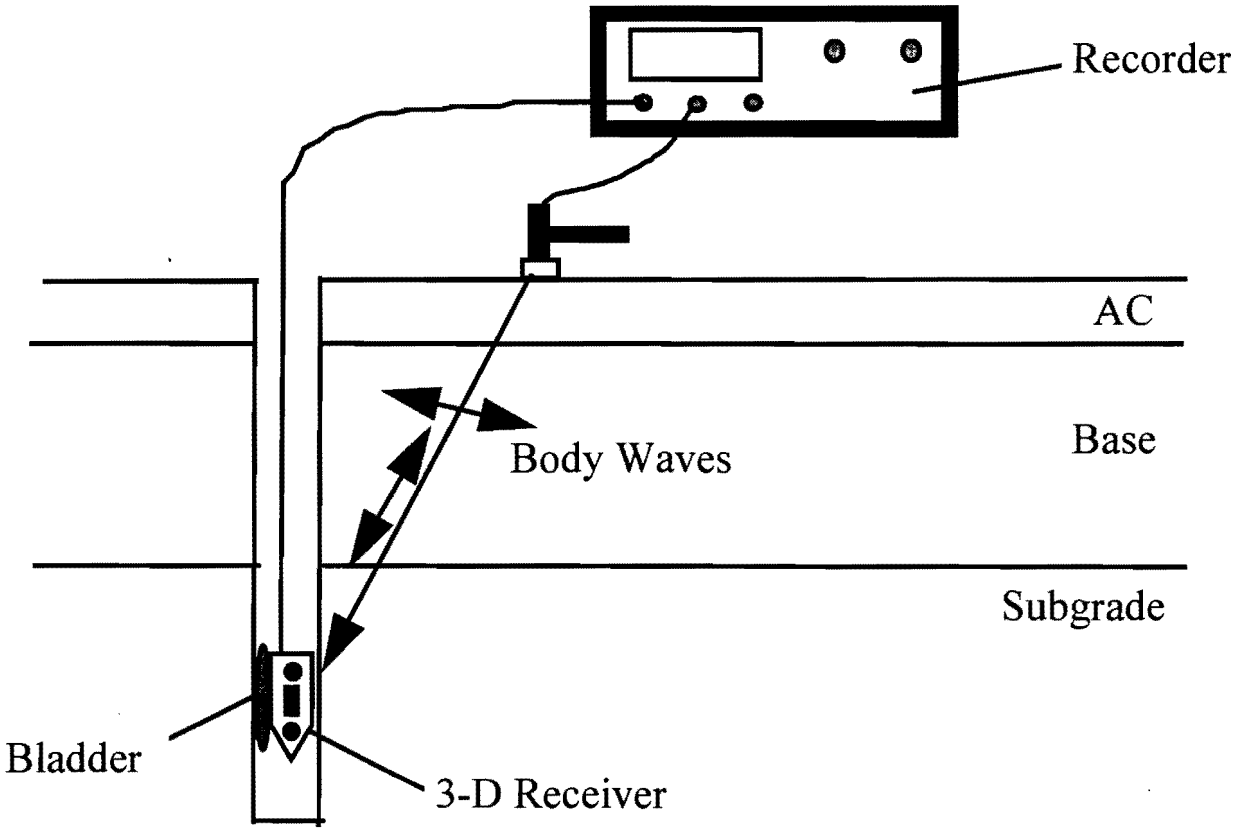

Figure 5 - Schematic of Downhole Seismic Tests

Compression waves (also called dilatational waves, primary waves, or P-waves) exhibit a push-pull motion. As a result, wave propagation and particle motion are in the same direction (see Figure 6a). Compression waves travel faster than the other types of waves, and therefore appear first in a direct travel-time record.

Shear waves (also called distortional waves, secondary waves, or S-waves) represent a shearing motion, causing particle motion to occur perpendicular to the direction of wave propagation (see Figure 6b). Shear waves travel more slowly than P-waves and thus appear as the second major wave type in a direct travel-time record.

The objective of tests with the SDCP is to identify the time at which different types of wave energy arrive at each sensor. The velocity of propagation, V, is calculated by dividing the distance between the source and the receiver, X, by the difference in the arrival time of a specific wave, t. In general, the relationship can be written in the following form:

$$V = \frac{X}{t} \tag{1}$$

In the equation, V can be the propagation velocity of any of the two waves (i.e., compression waves, V_P; or shear waves, V_S).

Propagation velocities per se have limited use in engineering applications. In pavement engineering, one is interested in Young's moduli of the different layers. Therefore, calculating the elastic moduli from propagation velocities is important.

Shear wave velocity, V_s, is used to calculate the shear modulus, G, by

$$G = \rho V_s^2 \tag{2}$$

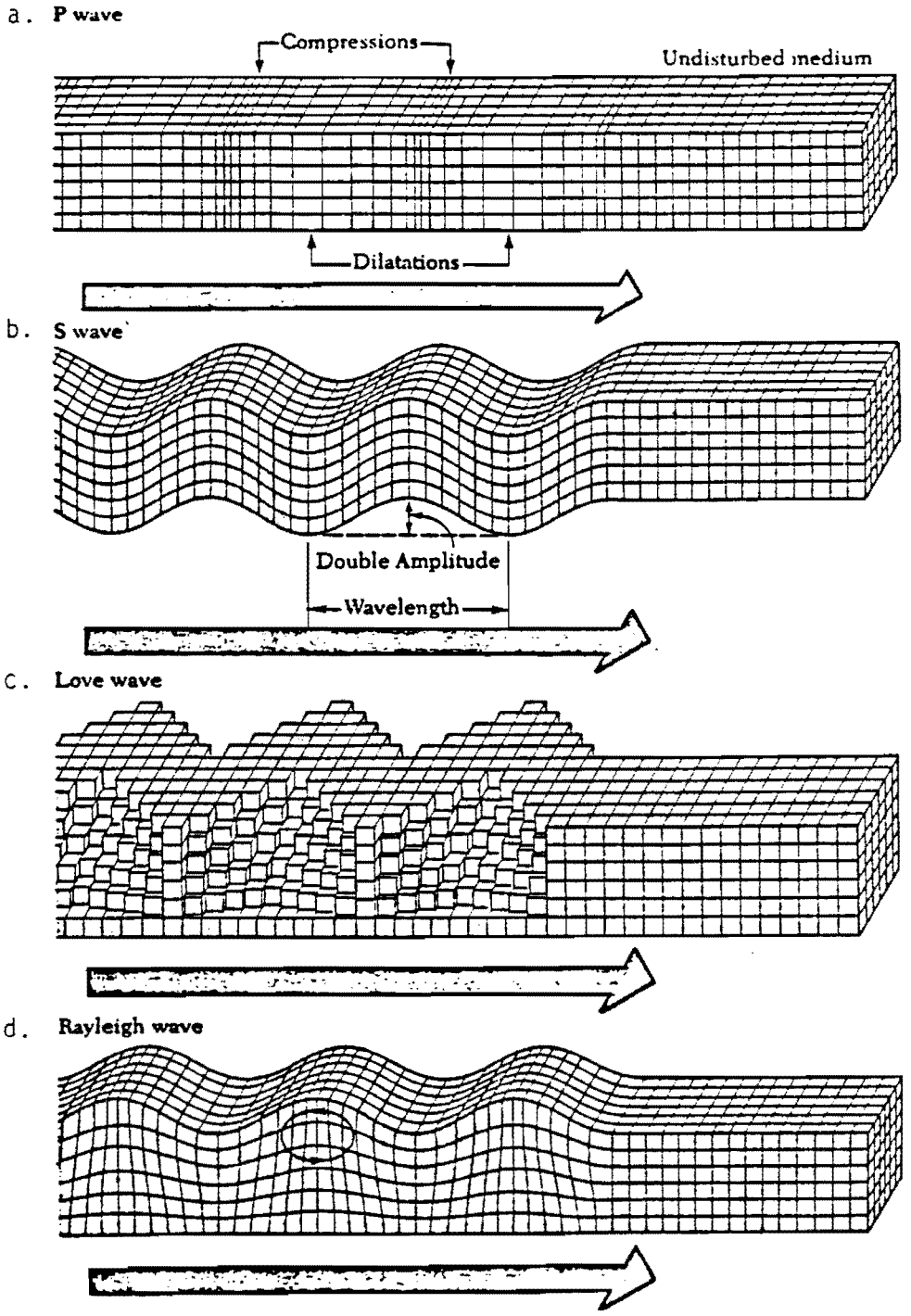

Figure 6 - Behavior of Seismic Waves

in which ρ is the mass density. If Poisson's ratio (or compression wave velocity) is known, Young's modulus, E, can be calculated from

$$E = 2G(1 + \nu) = 2\rho V_s^2(1 + \nu) \tag{3}$$

The Poisson's ratio, ν, used in the above equations can be readily determined using:

$$\nu = \frac{0.5\ \alpha^2 - 1}{\alpha^2 - 1} \tag{4}$$

where $\alpha = V_P / V_S$. (V_S and V_P are shear and compression wave velocities, respectively).

Typical time domain records from one Seismic DCP test are shown in Figure 7. Three records are shown in the figure. The bottom one is called the trigger record. The point when a sudden step change in voltage occurs corresponds to the impact of the pavement by the hammer as discussed before.

The two upper traces correspond to the records from a vertical accelerometer, and one of the horizontal accelerometers. Only two of the three records typically contain useful information. The third accelerometer, which is perpendicular to the direction of impact usually does not contain strong signals.

The arrivals of the waves are clearly marked on the figure. In each record an initial period with no appreciable amplitude can be observed after the activation of the trigger. This period corresponds to the time for a wave to propagate between the source and the receiver. The first excursion of the energy on each record, marked as P, corresponds to the arrival of compression waves. As indicated before, compression waves travel faster than other types of waves, and as such observed first on the record. The arrivals of shear waves, marked as S on the records, correspond to the initiation of a large amplitude, low energy on the record.

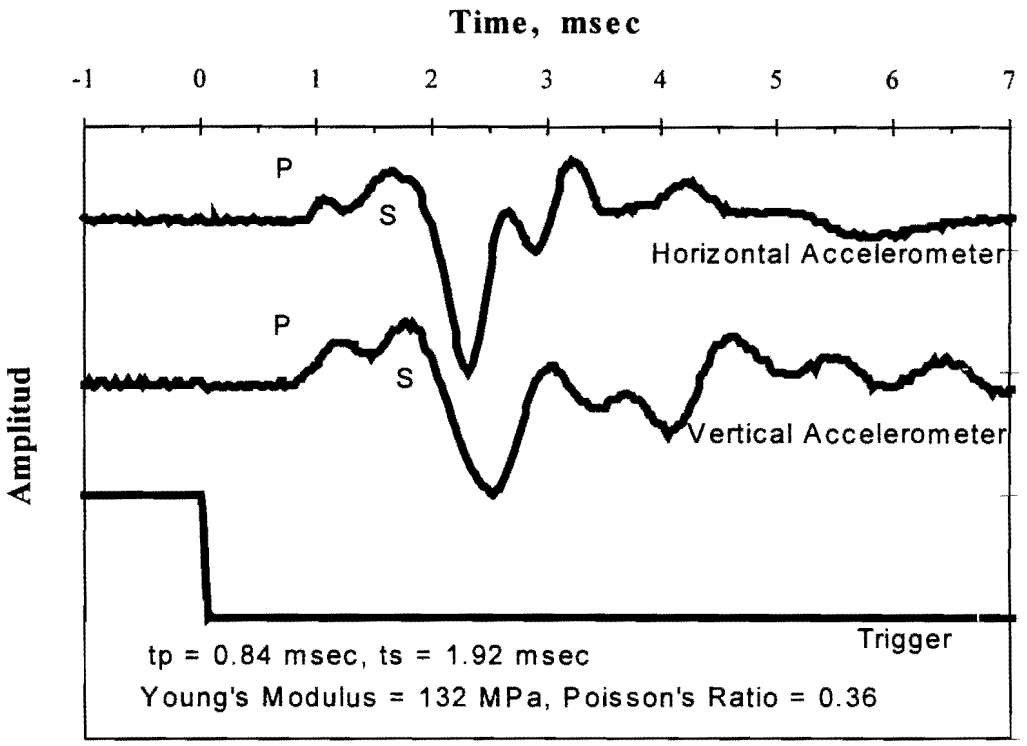

Figure 7 - Typical Time Records from Seismic DCP

In the records shown the arrivals of the waves from the two receivers concur quite reasonably. In this manner, one can determine the modulus and Poisson's ratio reliably. When the horizontal distance between the source and receiver is small relative to the depth at which the receiver is placed, waves predominantly propagate vertically. Alternatively when the source is located at large horizontal distances relative to the depth of the receiver waves propagate predominantly horizontally. In these cases, the energy associated with only one type of wave (shear or compression) will be dominant in each of the two records. That is the main reason that a three-dimensional accelerometer array is used.

The calculation of the modulus and Poisson's ratio using Equations 1 through 4 is also included in Figure 7. Once the traveltimes are identified, the determination of these parameters is rather simple.

Instrumented Dynamic Cone Penetrometer (IDCP)

One of the goals of this study was to obtain more quantitative results from the DCP. To achieve this goal, the anvil of the DCP was instrumented using an accelerometer and a load cell (see Figure 8). The load cell measures the energy imparted to the anvil, and the accelerometer is used to estimate the displacement experienced with the DCP.

The behavior of the DCP is quite similar to that of a standard penetration test (SPT) routinely used in geotechnical engineering field. Schemertmann and Palacios (1979) studied the distribution of energy in the SPT (see Figure 9). Upon the impact of the anvil with the hammer, kinetic energy will propagate in compression down the DCP rod. Upon arrival at the tip of the DCP, some of the energy is consumed to move the tip into the soil. The remainder of the energy reflects back and propagates upward as tensile energy. This process is repeated at the two ends of the DCP until the

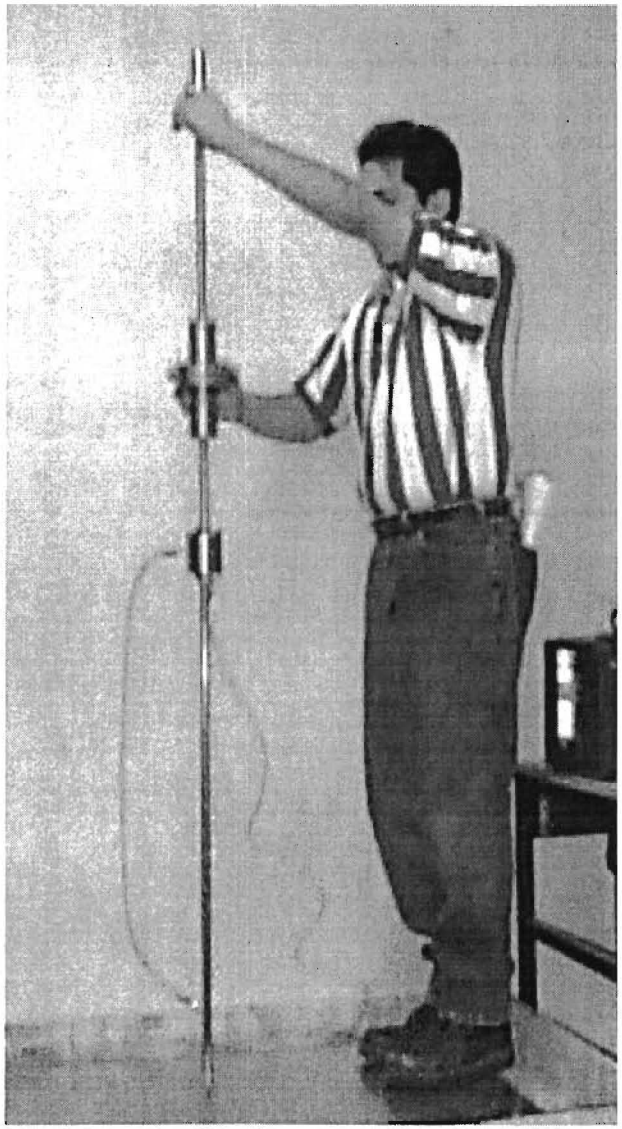

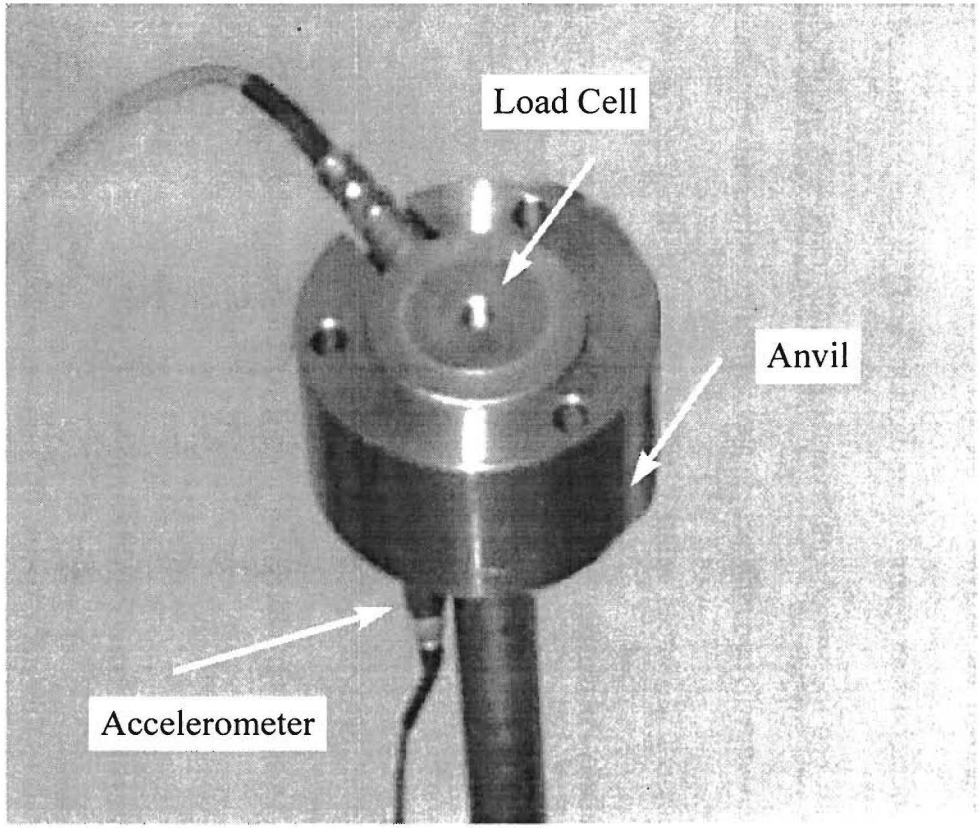

Figure 8 - Schematic of Instrumented DCP (IDCP)

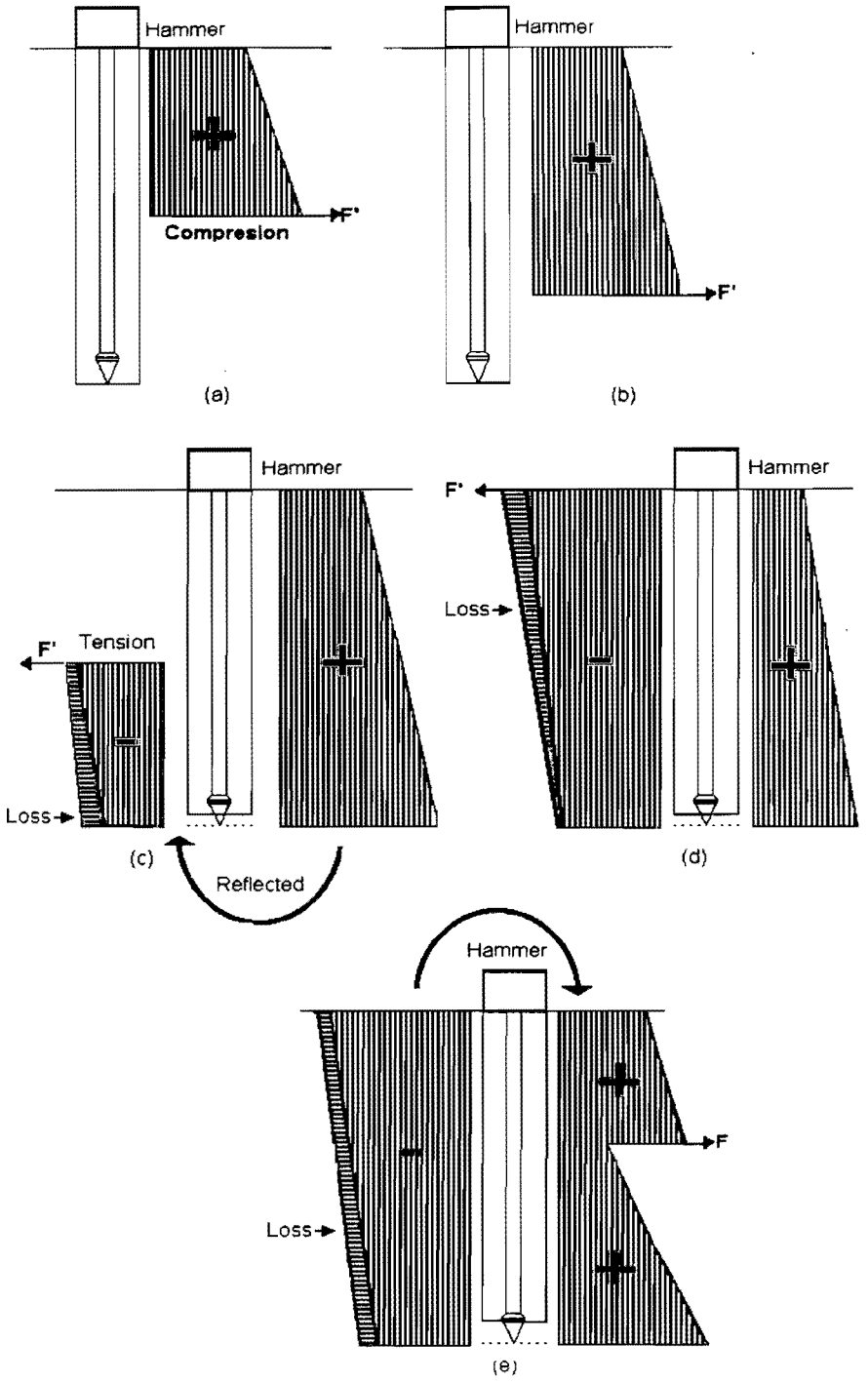

Figure 9 - Idealized Distribution of Energy in a DCP Rod

entire energy is dissipated. If the tip of the DCP is placed in a resistant-free material, all the energy will reflect back.

Typical load and acceleration from tests on a subgrade are shown in Figure 10. The initial half-sine energy lasting about 0.1 msec corresponds to the initial impact of the anvil. Other energy excursions correspond to the reflection of the energy from either the tip or the end of the DCP rod. To better visualize the results, it will be beneficial to convert the time axis to a normalized distance axis (see Figure 11). The velocity of propagation of waves in a steel rod such as one used in the DCP is about 4650 m/sec, and the length of the rod between the anvil and tip or the end of the DCP is about 98 cm. Therefore, it takes about 0.21 msec for the wave generated by the impact of the anvil to travel from the anvil to the tip of the DCP. By dividing the time axis with the 0.21 msec, one obtains the multiples of the length of the DCP between the anvil and the tip. In other words, a normalized distance of 1 corresponds to the time that it takes for the wave to travel from the anvil to the tip of the DCP.

From Figure 11, up to a normalized distance of 2, the acceleration and load follow each other quite well. However, at the normalized distance of 2, the load and acceleration demonstrate change in polarity. The load at that distance is negative indicating that the load cell is experiencing a tensile force; whereas the accelerometer is indicating a positive acceleration (i.e., the rod is moving down). This behavior can be reasonably described by the pattern of wave propagation within the rod. The initial impact generates a compressive load in the DCP rod which causes a downward motion of the rod. However, the wave that reflects upward from the DCP tip corresponds to a tensile load (see Figure 9). For an upward propagating tensile wave, the motion is downward. Therefore, at the

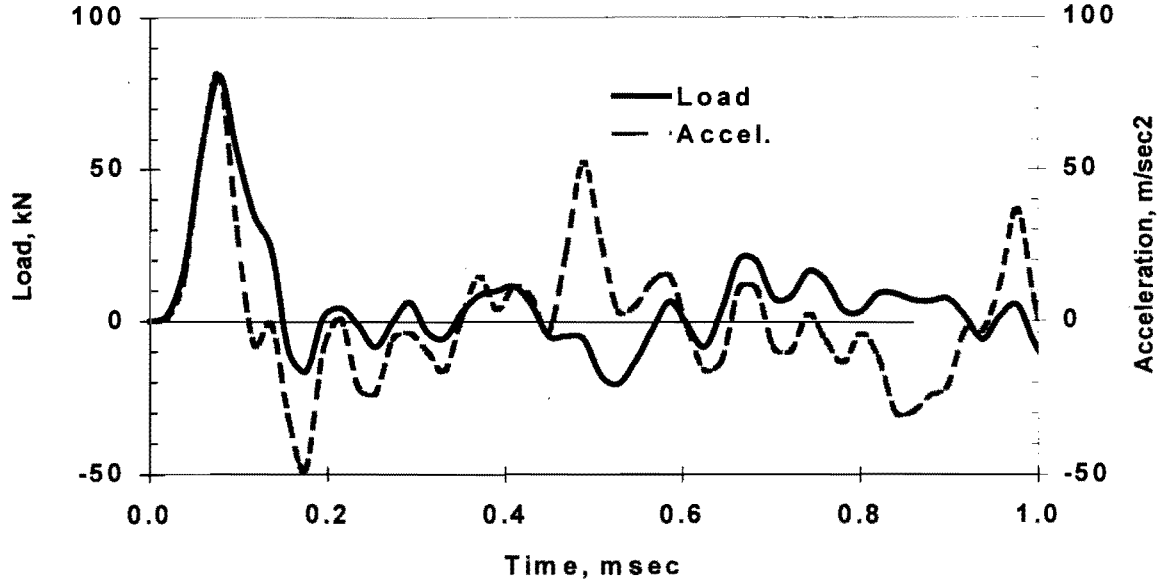

Figure 10 - Load and Acceleration Time Histories from a DCP Impact

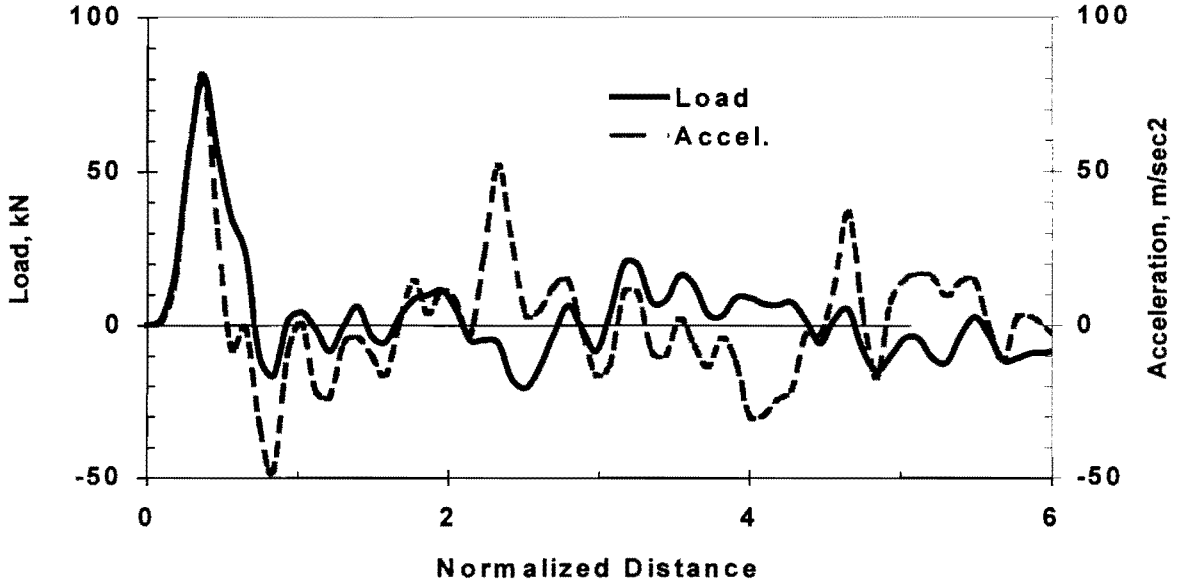

Figure 11 - Variation in Load and Acceleration with Distance along the rod.

normalized distance of 2, the round trip distance of the wave to the tip and back to the anvil, the scenario described above should occur. Such a pattern can be followed at other normalized distances as well.

The acceleration record shown in Figures 10 or 11 can be integrated once to determine the velocity, and the second time to determine the displacement. The variation in velocity with normalized distance is shown in Figure 12. The cyclic increase or decrease in velocity corresponds to the location of input energy at a given distance. The variation in displacement with normalized distance is shown in Figure 13. Due to impact, the displacement is ramping up in steps as the wave propagates in the rod. Even though not shown, at about a normalized time of 10, the rebound of the rod begins. The variations in velocity and displacement with distance quite nicely follow the theoretical pattern required for this type of test.

Finally, the variation in kinematic energy with time (or normalized distance) can be calculated (see Figure 14). The energy at a given time, E(t), can be calculated from

$$E(t) = \int_0^t F(t)\ V(t)\ dt \qquad (5)$$

where F(t) and V(t) are the force and velocity. The energy, as shown in Figure 14, gradually increases to a constant value, and more or less remains at that level.

The energy determined in this manner corresponds to the energy propagating in the rod. Therefore, any energy that consumed to penetrate the rod into the soil is not considered. One way to determine the amount of energy that is absorbed by the soil is to determine the energy in the DCP system under a "free" condition. In the "free" condition, when the DCP tip is not encountering any

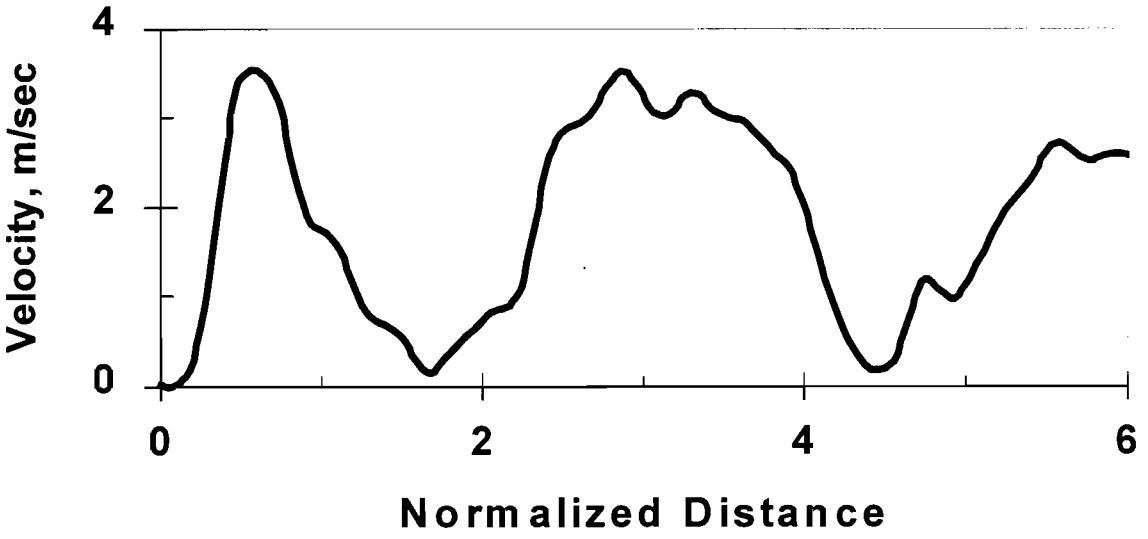

Figure 12 - Variation in Particle Velocity with Distance

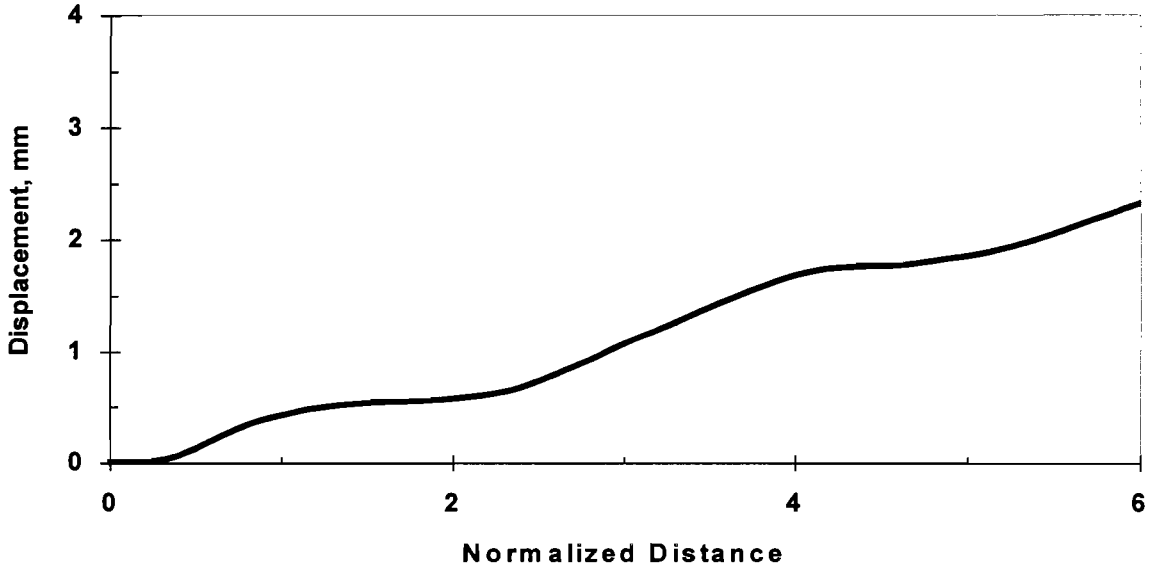

Figure 13 - Variation in Displacement with Distance

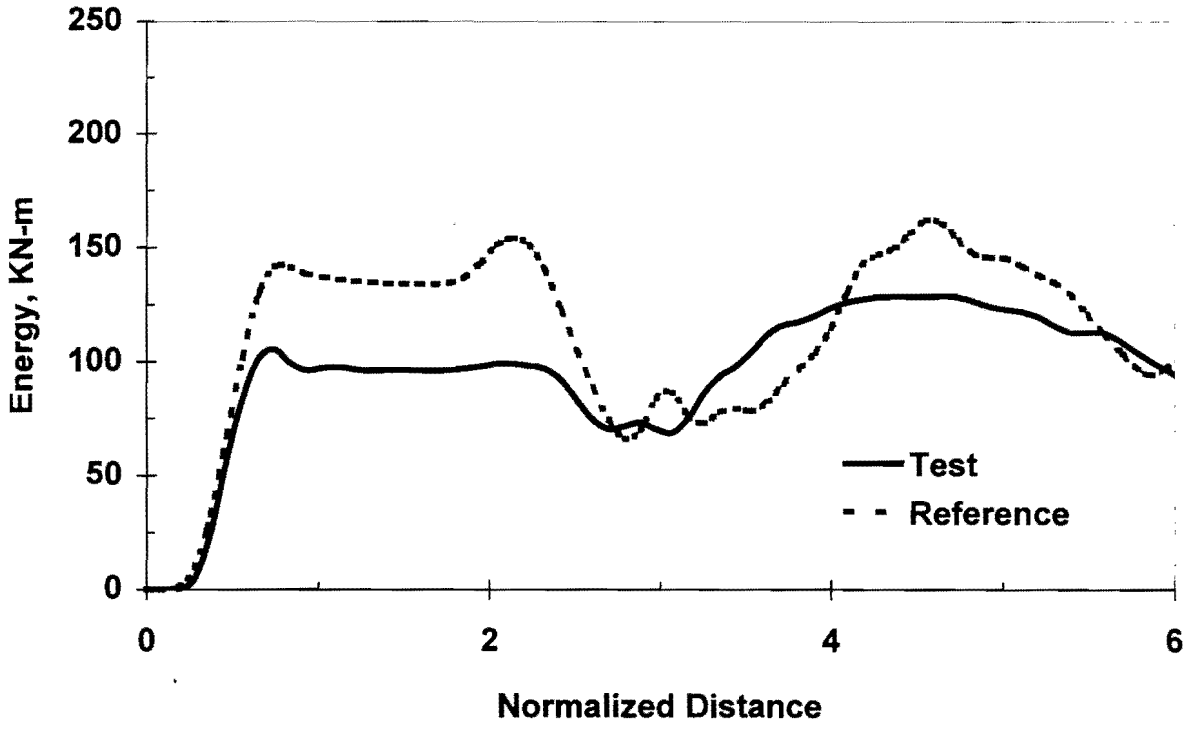

Figure 14 - Variation in Energy with Distance within the Rod

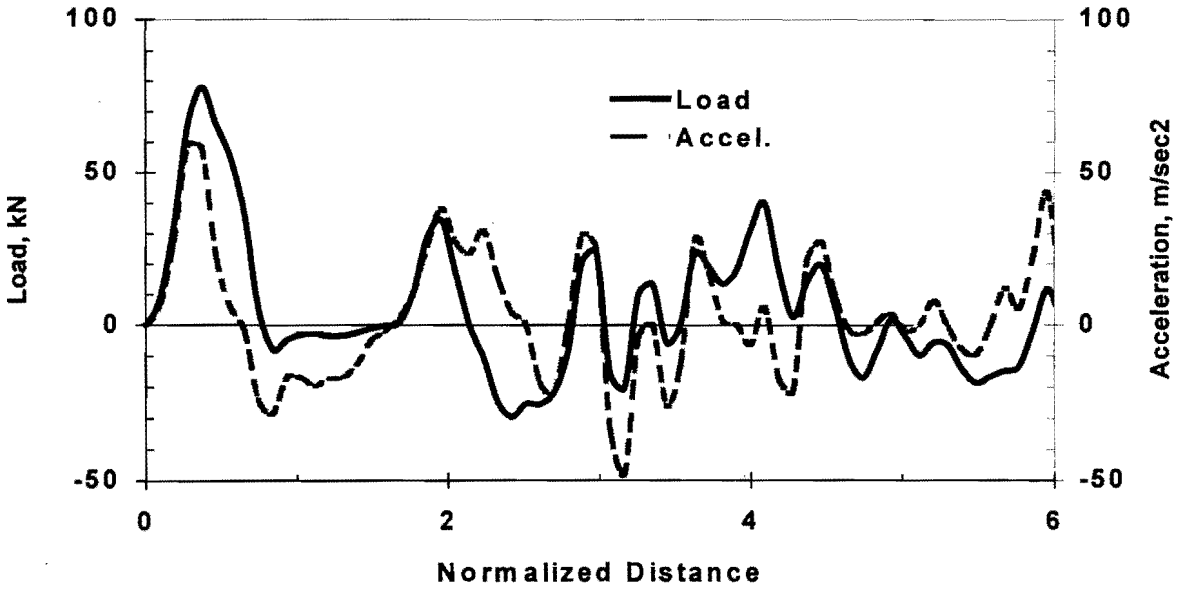

Figure 15 - Variation in Load and Acceleration with Distance for Free Condition

resistance, all the energy imparted to the rod remains in the rod. The energy in this condition can be estimated from numerical analysis or through a calibration process.

In this study we chose a calibration process because of its practicality and ease. To determine the behavior of the system under free condition, we placed it on top of a bucket filled with about 30 cm of very loosely packed foam, and performed a test. The response of the DCP was recorded under the exact setup used in the field. By comparing the behavior of the DCP during the field test with the free condition one can delineate the amount of work and energy that has gone toward penetrating the DCP into the soil. The measured load and acceleration from the free condition are shown in Figure 15. The main features of the results shown in Figure 11 are applicable here with minor variations.

The variation in energy from the free condition (marked as reference) is compared with the energy from an actual test in Figure 14. The difference in the energy from the two curves corresponds to the energy transmitted into the soil.

Finally the soil resistance, R(t), can be determined from

$$R(t) = \frac{\Delta E}{d\ A} \tag{6}$$

Assuming that all the resistance is due to the tip penetration, an average "strength" can be determined from Equation 6. Parameter ΔE is the energy loss (i.e., difference in energy between the reference condition and the energy from the point tested). Parameter A is the effective area associated with the DCP test. One problem that requires further study is the determination of the appropriate area. In this study, as a first approximation, we chose to use the cross-sectional area of the DCP. Parameter d is the penetration distance of the DCP tip.

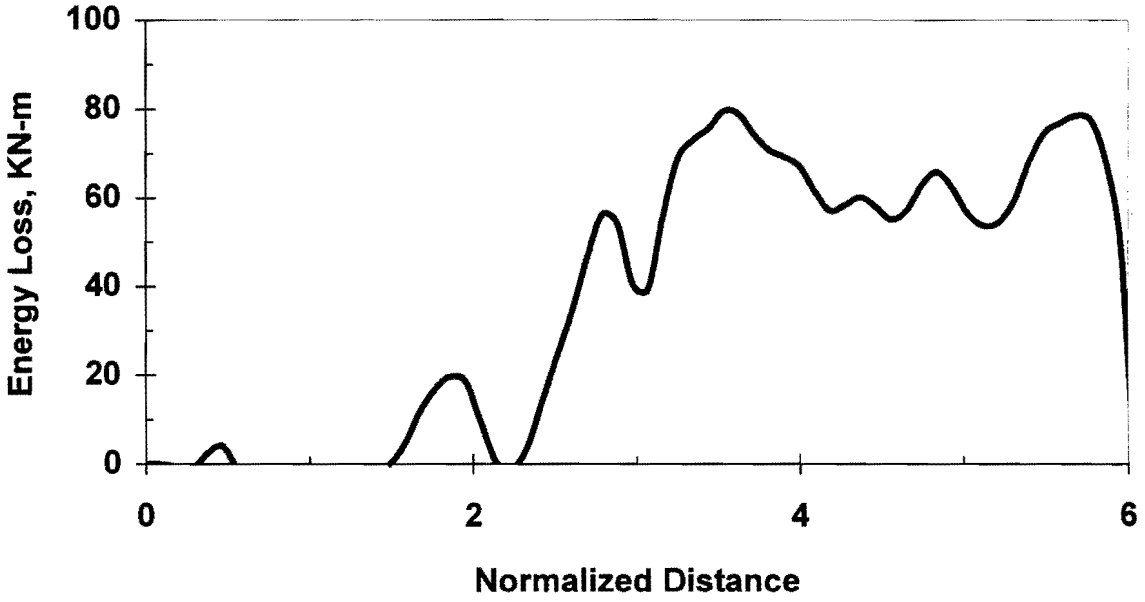

Figure 16 - Variation in Energy Loss with Normalized Distance

A typical energy loss with normalized distance is shown in Figure 16. Once again, there is a gradual increase in the energy loss up to a normalized distance of 4; after that the energy loss is more or less constant. We chose the loss in energy after a normalized distance of about 4 as the parameter to be used in this study. Further analytical and experimental studies are required to better justify this assumption. In summary, this is a simple but approximate method of calculating the resistance. More rigorous methodology is under development.

Seismic Pavement Analyzer (SPA)

UTEP, in cooperation with TxDOT and SHRP, has developed a trailer-mounted device called the Seismic Pavement Analyzer (see Figure 17). The details of the device are fully covered in UTEP Report 1243-1 (Nazarian et al., 1995).

Five different tests can be carried out with the SPA:

1. Spectral Analysis of Surface Waves (SASW),
2. Impulse Response (IR),
3. Ultrasonic Body Wave (UBW),
4. Ultrasonic Surface Wave (USW), and
5. Impact Echo (IE).

The SASW method is a seismic method that can nondestructively determine modulus profiles of pavement sections. The method provides the modulus and thickness of different layers. A computer algorithm utilizes the time records to determine a representative dispersion curve in an automated fashion. The last step is to determine the elastic modulus of different layers through an inversion process, given the dispersion curve.

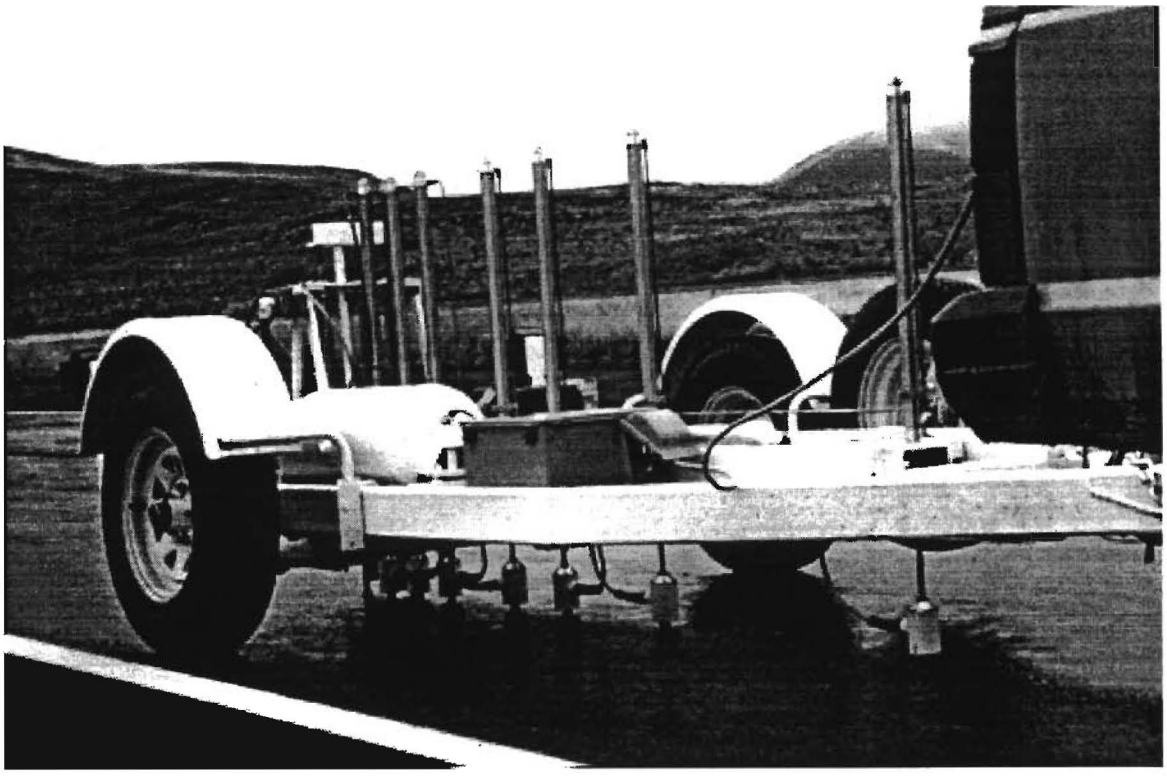

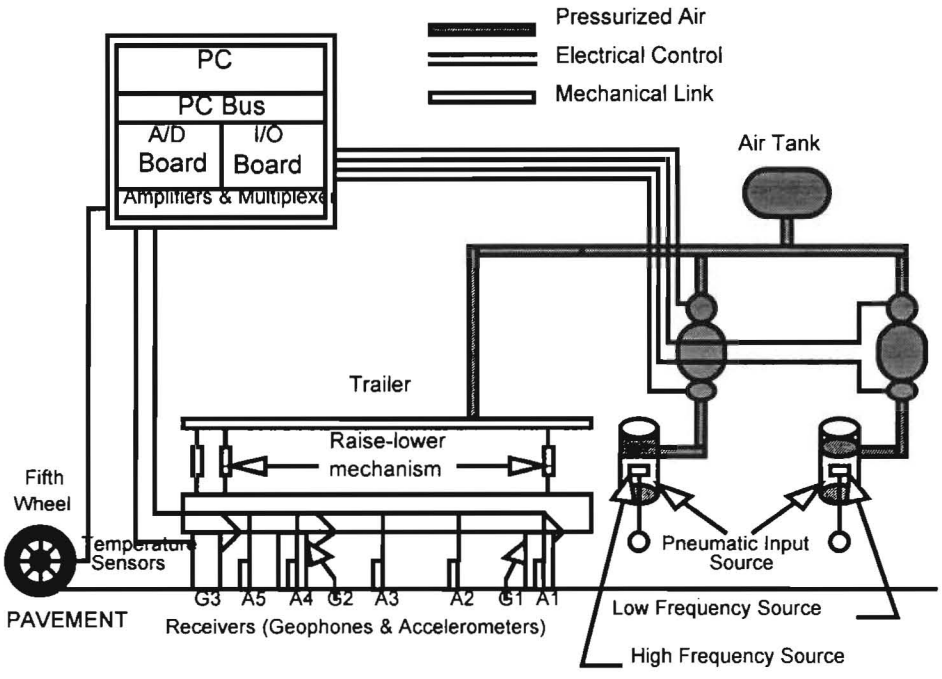

Figure 17 - Schematic of Seismic Pavement Analyzer

The main parameter obtained on flexible pavements with the impulse-response (IR) method is an overall stiffness of the pavement, which can be used to delineate between good and poor support.

The ultrasonic-body-wave and ultrasonic surface wave methods can directly measure Young's modulus of the top layer (AC or PCC). Since the sections tested are not covered with any of these materials, these two methods were not used.

The impact-echo method can be used to determine the thickness of a thick AC and PCC layers as long as the layer is thicker than 10 cm. Once again, since these conditions did not exist at the sites, this method was not used.

Presentation of Results

In this section, the results from tests at the seven sites in Bryan District are included. The sites are first introduced. Modulus profiles from the SPA are presented. The results from the IDCP and SDCP along with the moduli from SPA tests at those points are then compared.

Description of Sites

Seven preselected sites were extensively tested in July 1997. The sites covered a variety of base and subgrade conditions. A detailed description of the sites can be found in Report 3903-1 submitted by TTI. The location of each site is included in Table 1. Different sites had different characteristics and were stabilized with either cement or lime. The exact nature of the sites tested and as built properties were not available at the time of the report preparation.

At each site, the SPA was used at about 20 points. These points were also tested with the FWD and Dynaflect. The results from SPA tests at each site are summarized in Appendix A.

Average moduli of base and subgrade are included in Table 2. On the average, all bases seem to be reasonably stiff. However, the large coefficient of variation reported in Table 2 for each site indicates that the material is highly variable.

Table 1 - Location of Sites Tested

Site No.	C-S-J	Road	County	Length, Km
1	1147-01-020	FM 977A	Leon	3.2
2	1147-03-008	FM 977B	Leon	7.2
3	1147-03-010	FM 977C	Leon	5.1
4	2848-01-003	FM1124	Freestone	2.9
5	2619-01-xx	FM1935	Washington	3.2
6	N/A	FM2446	Robertson	1.6
7	N/A	FM2780	Washington	12.8

Table 2 - Overall Results from SPA

Site No.	Road	Average Modulus from SASW Tests, MPa*		Effective Stiffness from IR Test
		Base	Subgrade	
1	FM 977A	4075 (41%)	353 (53%)	672 (45%)
2	FM 977B	1551 (52%)	569 (50%)	1044 (25%)
3	FM 977C	3122 (36%)	207 (53%)	597 (42%)
4	FM1124	2900 (44%)	295 (39%)	834 (41%)
5	FM1935	3129 (47%)	241 (60%)	662 (40%)
6	FM2446	2535 (55%)	276 (30%)	523 (45%)
7	FM2780	2932 (65%)	325 (45%)	481 (60%)

** Number in parentheses corresponds to the coefficient of variation*

Average subgrade moduli estimated at different sites, as reflected in Table 2, are indicative of soft to average subgrade. Once again, the large coefficients of variations correspond to large point-to-point variability of the profiles measured.

The effective stiffness values from impulse response tests, which correspond to the overall condition of the pavement, are also reported in Table 2. Based on our experience, the average values reported corresponds to average pavement sections. However, the large coefficients of variation indicate that most sites should experience localized areas that are in fair to poor condition.

Young's moduli measured for the base and subgrade from the SPA specifically performed at the location of the DCP tests are included in Table 3. Also, included in the table are the moduli obtained with the seismic DCP. The schematic of test procedure with the SDCP at each site is shown in Figure 18a. The tip of SDCP was placed at a given depth, and the source point was then moved at 10 cm increments away from the borehole until a distance of about 50 cm. In that manner, the modulus of the layer can be reliably determined. After the SDCP is situated in the borehole, data collection takes about one minute.

If tests are performed in the subgrade, the traveltime has to be corrected so that the effects of the base and AC layers can be removed. Figure 18b clearly demonstrates this phenomenon. The farther the source is from the receivers, the longer the travelpath of the wave in the overburden material. The correction for the travel path is a simple geometry problem which is done in an excel worksheet.

The moduli obtained for the base using the SDCP and the SPA are in reasonable agreement except for FM 1935 that they differ by about a factor of two (see Table 3). One should have in mind that test with the DCP is extremely localized; whereas the SPA provides the properties over a range up to about 2 m. Also, one should be aware of the limitations in both methods in terms of data

Table 3 - Comparison of Parameters measured with the SPA, Seismic DCP, and Instrumented DCP

Site No.	Road	Young's Modulus, MPa				Soil Resistance from IDCP, MPa		Poisson's Ratio from SCDP		Overall Stiffness from IR, MPa
		Base		Subgrade		Base	Subgrade	Base	Subgrade	
		SPA	SDCP	SPA	SDCP					
1	FM 977A	4106	4381	286	394	--	62±8	0.19	0.21	560
2	FM 977B	2215	1980	480	--	--	195±75	0.38	--	1313
3	FM 977C	2923	3138	165	684	--	40±21	0.36	0.19	892
4	FM1124	1143	2315	197	254	204±125	36±36	0.29	0.22	324
5	FM1935	2286	1653	214	--	226±72	51±27	0.28	--	522
6	FM2446	1048	836	374	--	--	25±16	0.36	--	287
7	FM2780	559	573	142	--	62±4	10±2	0.30	--	184

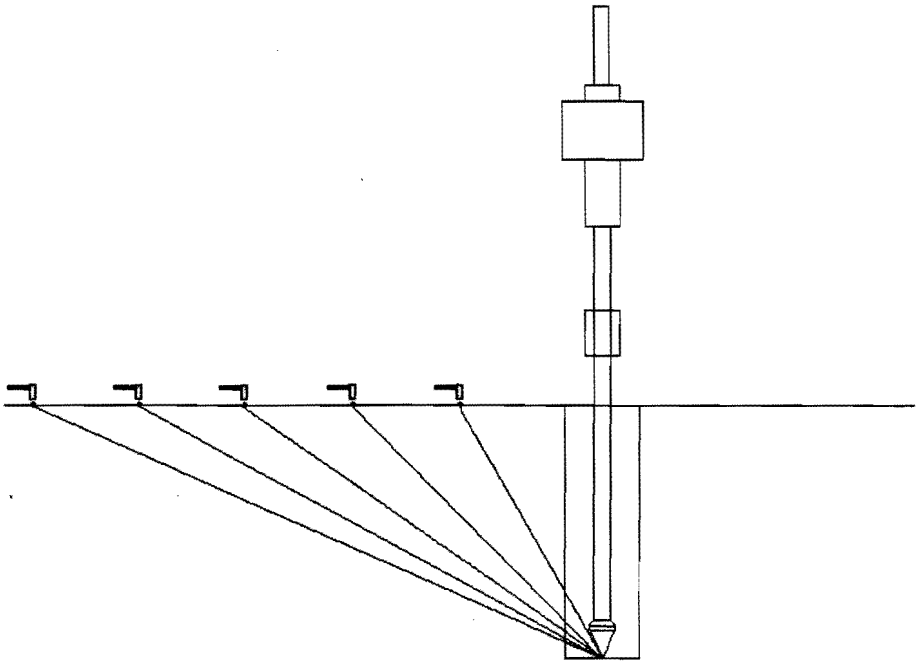

(a) Test Set Up

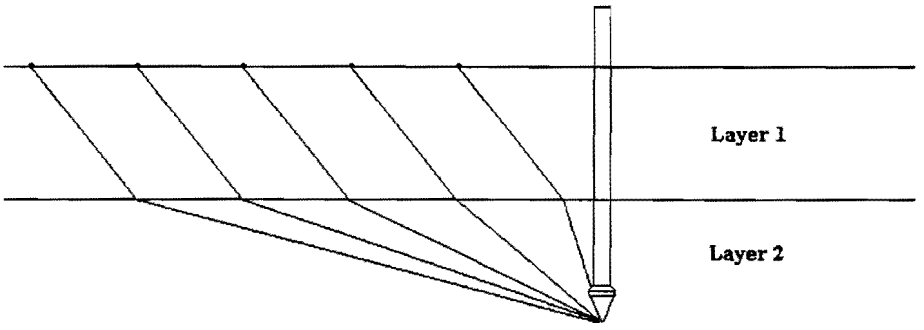

(b) Actual Ray Paths In Subgrade

Figure 18 - Test pattern with SDCP in Bryan District

reduction. For the SPA this includes errors in the inversion process and approximations in the construction of the dispersion curve, and for the SDCP is the inaccuracies in identifying the arrivals of different waves, and the approximations in correcting for raypath.

Because of the time limitation, the SDCP tests were carried out only on four subgrades. For one site (Site 2 in Table 3), the measurements were corrupt and could not be reduced. In the other three cases, the moduli from the SDCP are larger than the moduli from the SPA. This can be due to the fact that the SPA provides a subgrade modulus that corresponds to a depth down to 1.5 m; whereas, the SDCP tests were performed very close to the base. The locations of the tip of the SDCP as a function of layering at sites is shown in Figure 19. For Site 1, the SDCP is about 20 cm within the subgrade. The tip of the SDCP for Site 3 is only 5 cm within the subgrade, and for Site 4 is about 15 cm within the subgrade. It seems that the deeper the SDCP is placed within the subgrade, the smaller the difference in moduli from the two methods will become. For example, for Site 3, the difference in moduli is about a factor of two. For the other two cases where the SDCP was located deeper into the subgrade, the moduli from the two methods are closer. From this study, it seems that tests should be performed deeper into the subgrade.

The Poisson's ratio of each layer is reported in Table 3. Even though a convenient independent way for verifying the Poisson's ratios does not exist, they seem reasonable for the types of material tested. As indicated before, this is the only method at this time that can conveniently provide Poisson's ratio.

The moduli measured with the IR tests (see Table 3) can be used as an overall stiffness parameter. These values are affected by the moduli of the base and subgrade as well as any shallow rigid layer below the pavement. The overall stiffness can be used to delineate weak sections from strong sections.

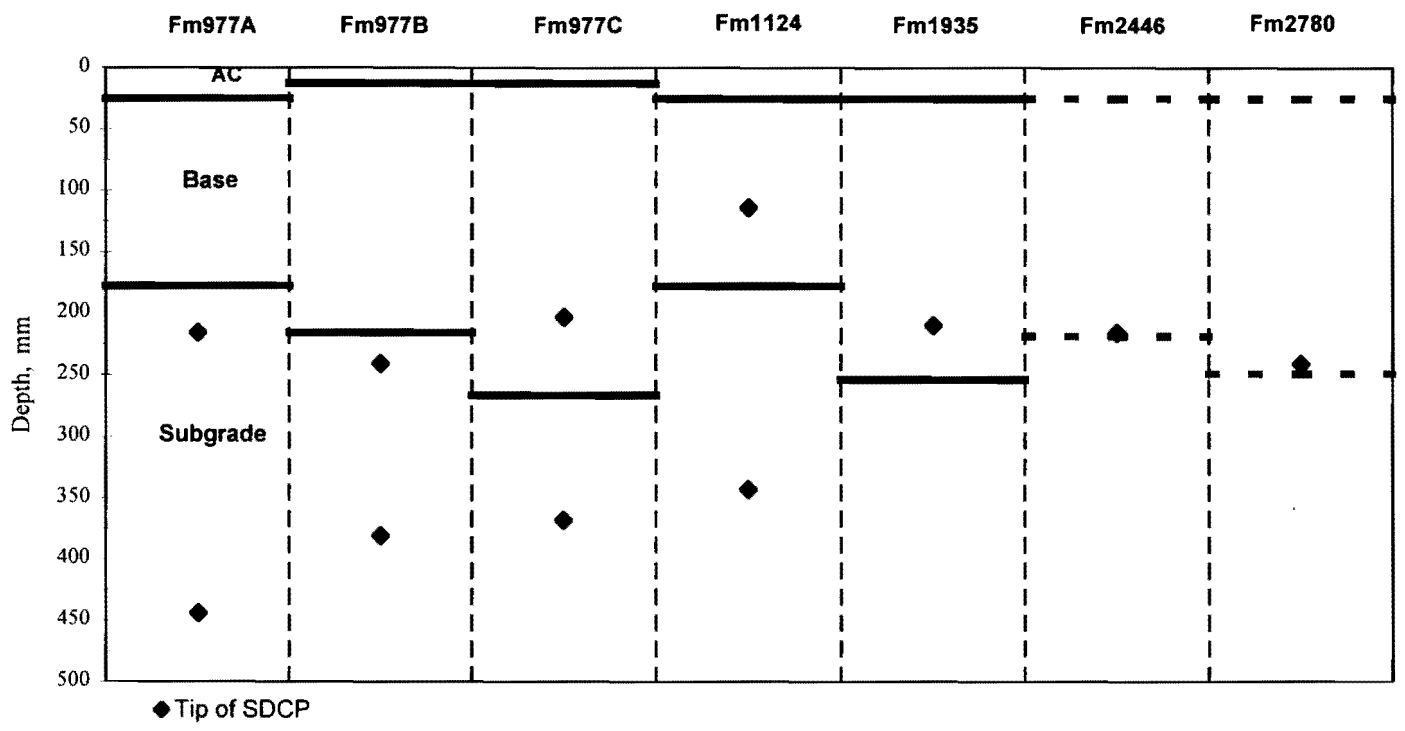

Figure 19 - Location of the Tip of SDCP at Different Sites

Extensive tests with the instrumented DCP were also carried out. At each site, more or less about a dozen measurements were made. A test consisted of penetrating the IDCP about 25 to 50 mm and then recording the output of the load cell and accelerometer as discussed before. In some instances, the base was too stiff to be penetratable with the IDCP. Therefore, in those cases, tests were not carried out.

The variation in energy loss with the rate of penetration from about seventy test points collected in this study is shown in Figure 20. A reasonably unique relationship between the two parameters can be observed. The slope of the curve for penetration rates below 20 mm/blow is quite steep. This indicates that for stiff materials the relationship between the energy absorbed by the soil and the penetration rate is well defined. For higher penetration rates, the curve becomes relatively flat indicating that for very soft subgrades the soil resistance is less dependent on the penetration.

The soil resistance as a function of penetration rate is shown in Figure 21. The relatively unique relationship between these two parameters is rather impressive. However, the magnitude of the resistance in the curve seems rather high. This can be due to the approximations introduced in determining the resistance from the energy loss described before, and perhaps it may be due to the method of calibration of the IDCP used. Both of the two areas require further improvement.

The average soil resistance for each material tested is reported in Table 3. The values correspond to the average along the thickness of the layer. Therefore, a large standard deviation is measured for each case. For the base layer, a quite reasonable trend between the modulus of the base (from either the SPA or the SDCP) and the soil resistance measured with the IDCP. The same trend is also observed for most subgrades.

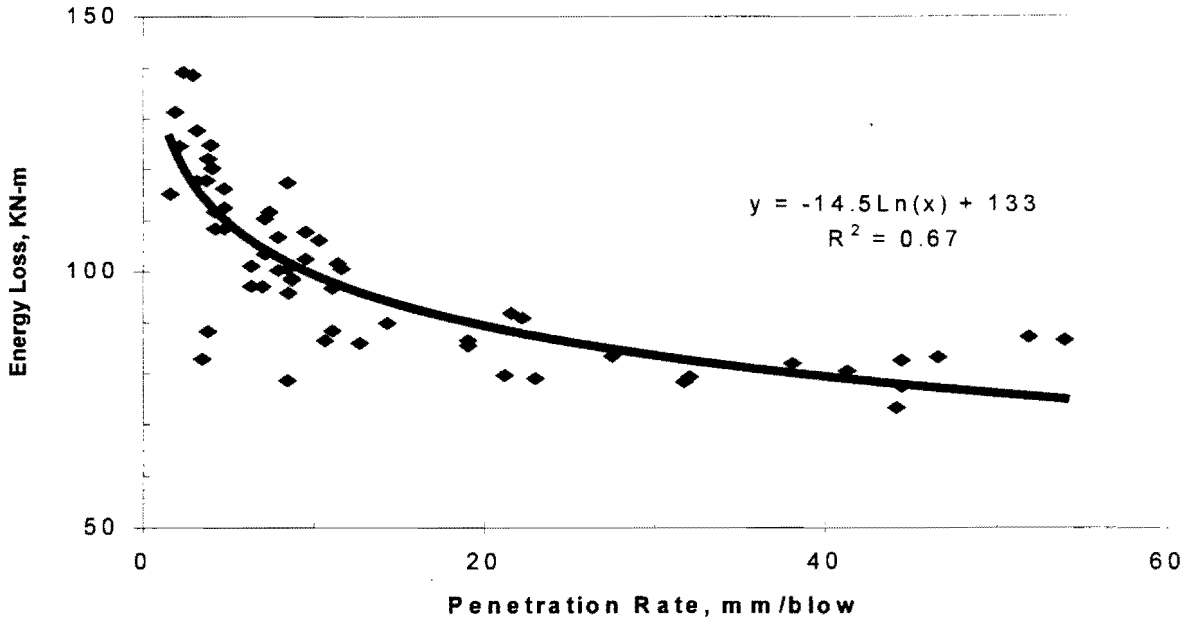

Figure 20 - Variation in Energy Loss with the Rate of Penetration of IDCP

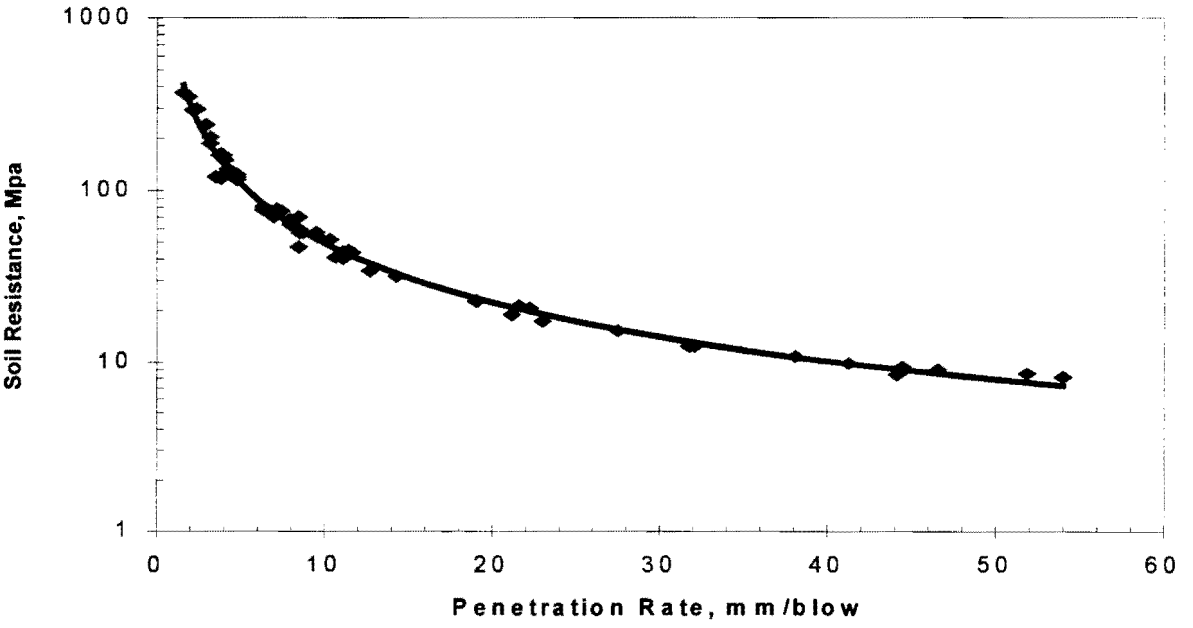

Figure 21 - Variation in Soil resistance with the Penetration Rate for IDCP

Overall, it seems that the prototype of the IDCP provides valuable information. However, a better method for calibrating the system and some experimental and analytical work is still needed to improve the results from the device.

Closure

In this report the results from developing two new improvements to the Dynamic Cone Penetrometer (DCP) are included. In the first case, a three-dimensional accelerometer package was retrofitted inside the tip of a device that can occupy holes that are slightly larger than the DCP holes. With this device, the modulus of base and subgrade can be potentially determined.

The second improvement consisted of adding a load cell and an accelerometer to the anvil of an actual DCP so that the load and deformation of the device during penetration can be determined. Such information can be translated to the soil resistance and potentially soil strength during field tests.

The devices were used at seven sites for validation and evaluation. Based on those results, both devices have shown good potential for being useful. In most cases, the moduli obtained with the seismic DCP were in good agreement with moduli obtained with the SPA. A better field set up is needed to minimize the influence of the base on the modulus of the subgrade. The instrumented DCP showed promise as well. A very good relationship between the rate of penetration and soil resistance was found. However, the soil resistance values reported seem higher than expected for the materials tested. A better calibration process, and a rigorous analytical process are needed to understand the reason for high resistance.

Further development of these devices is recommended as they have the potential for providing more quantitative results as compared to the existing DCP tools.

References

1. Kleyn E.G. and Savage P.F. (1982) "The Application of the Pavement DCP to Determine Bearing Properties and Performance of Road Pavements," Proceedings, International Symposium on Bearing Capacity of Roads and Airfields, Trondhiem, Norway.
2. Linveh M., Ishai I. (1985) "Evaluation of Flexible Pavements and Subsoils Using the South African Dynamic Cone Penetrometer," No. 85-301, Transportation Research Institute, Technion, Haifa, Israel.
3. Nazarian S., Yuan D., and Baker M. (1995), "Rapid Determination of Pavement Moduli with Spectral-Analysis-of-Surface-Waves Method," Research Report 1243-1, The University of Texas at El Paso, 76 p.
4. Schemertmann J.H., and Palacios A. (1979), "Energy Dynamics of SPT," Journal of Geotechnical Engineering Division, ASCE, Vol 105, No. GT8.
5. Shinn J.D., Timian D.A., Smith E.B., Morlock C.R., Timian S.M., and McIntash, D.E. (1988), "Geotechnical Investigation of the Ground-Based Free Electron Laser Facility, "Report ARA-NED-88-10, Applied Research Associates, South Royalton, VT.
6. Webster S.L., Grau R.H., and Thomas P.W. (1992) "Description and Application of Dual Mass Dynamic Cone Penetrometer," Report GL-92-3, Army Corps of Engineers, Waterways Experiment Station, Vicksburg, Mississippi.
7. Woods R.D. (1991) "Field and Laboratory Determination of Soil Properties at Low and High Strains (state of the art paper)," Proceedings, 2nd International Conference on Recent Advances in Geotechnical Earthquake Engineering and Soil Dynamics, St Luis, Missouri

Appendix A

Variation in Properties from SPA at Seven Sites

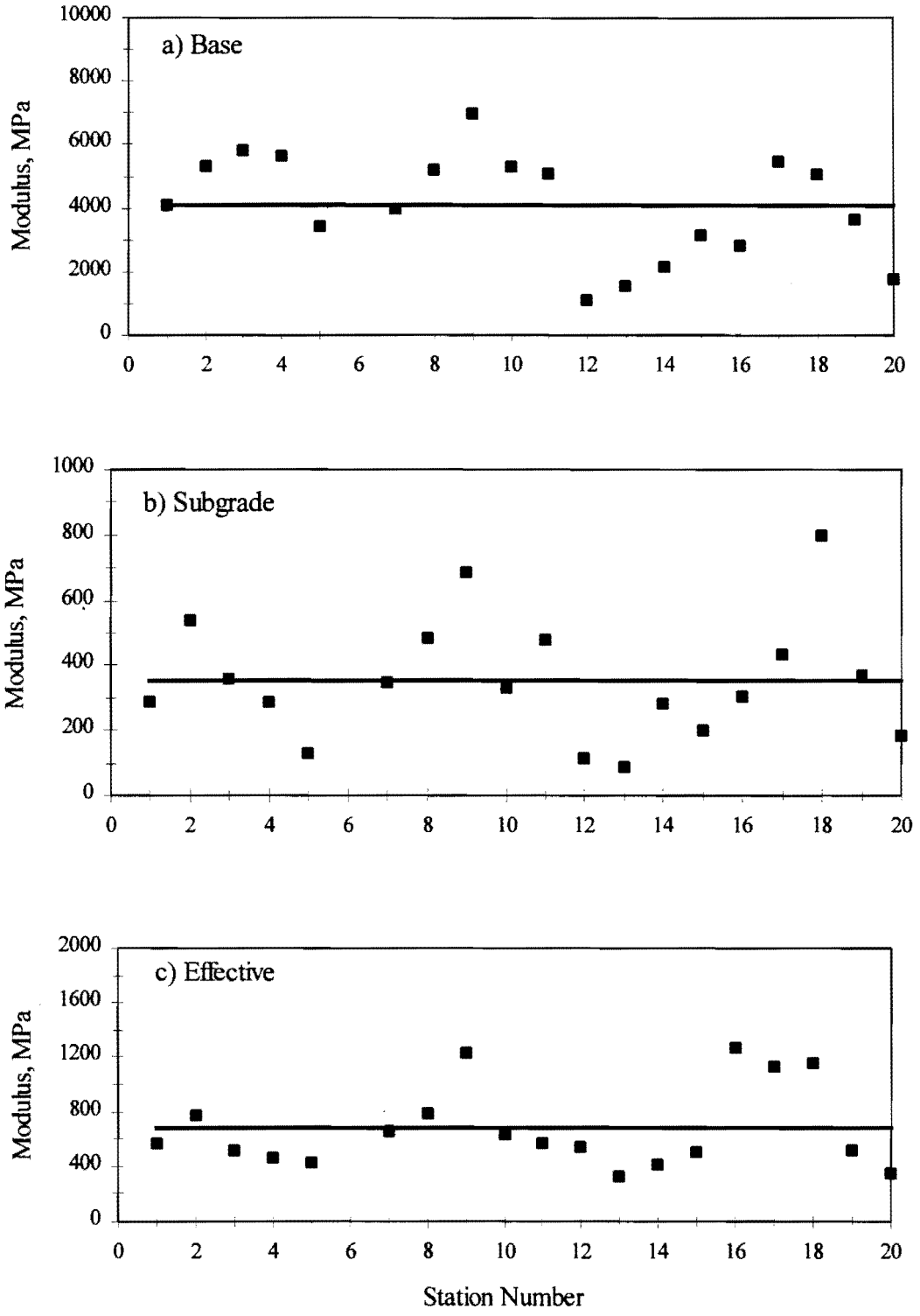

Figure A1 - Results from SPA Tests at FM 977A

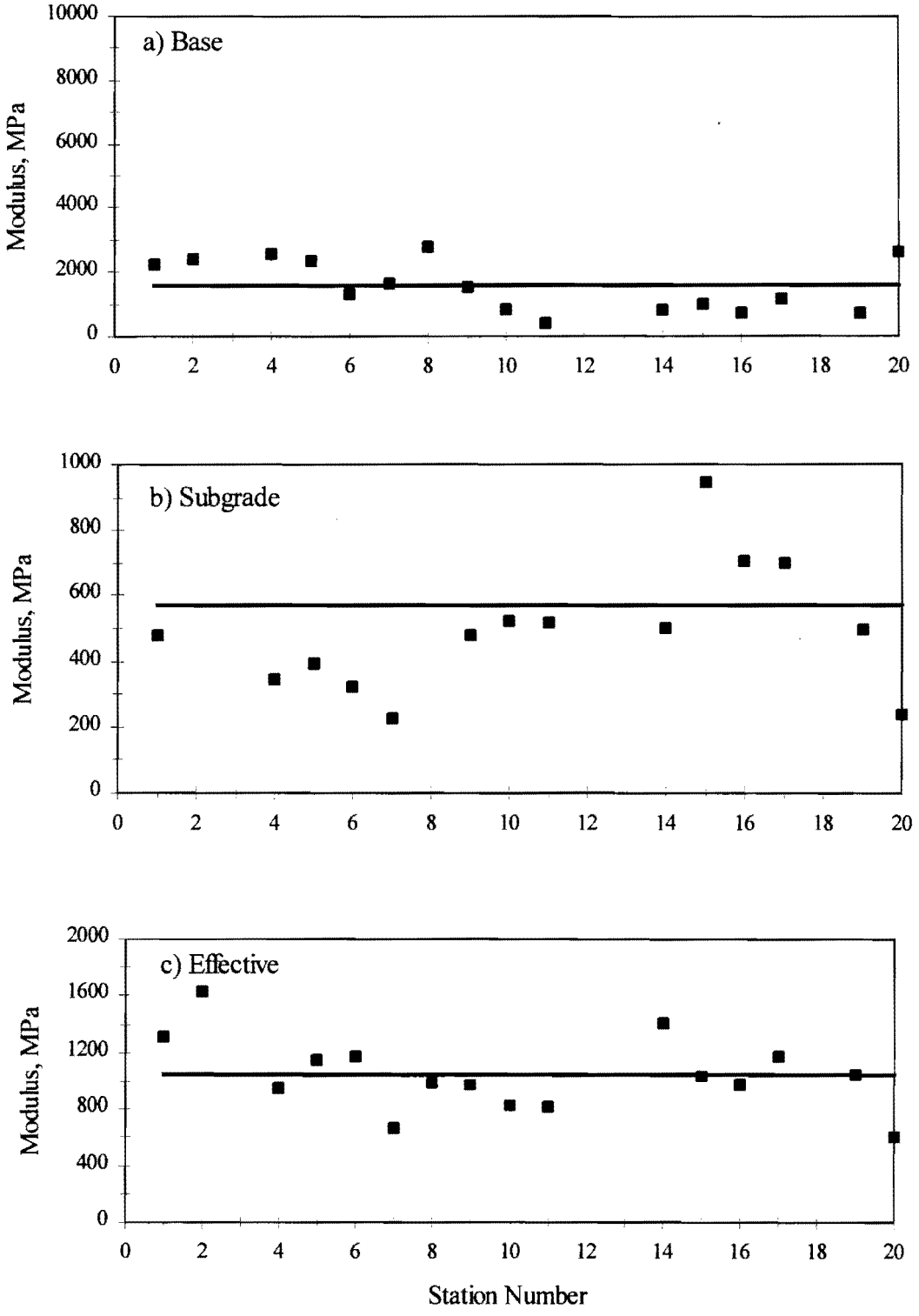

Figure A2 - Results from SPA Tests at FM 977B

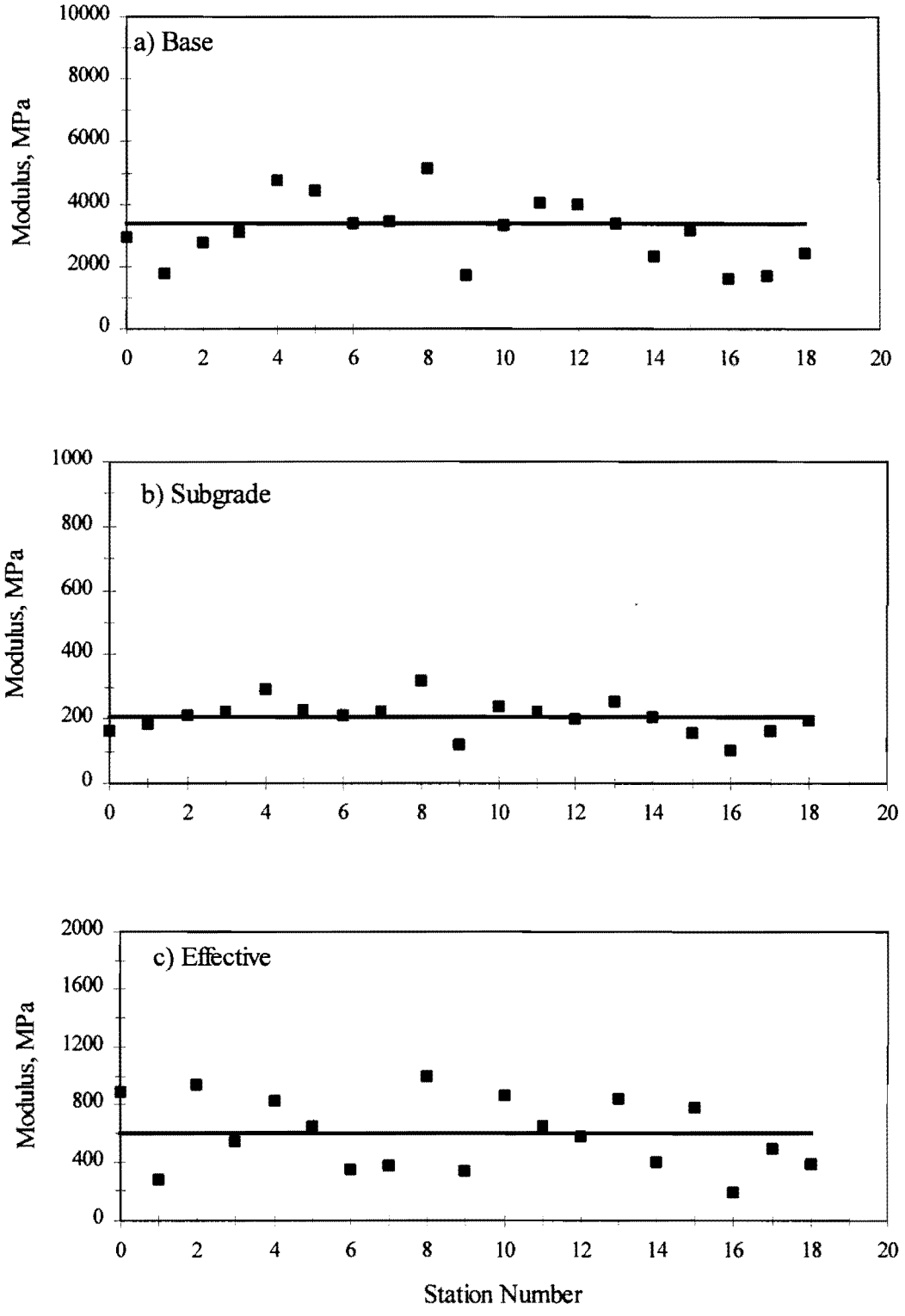

Figure A3 - Results from SPA Tests at FM 977C

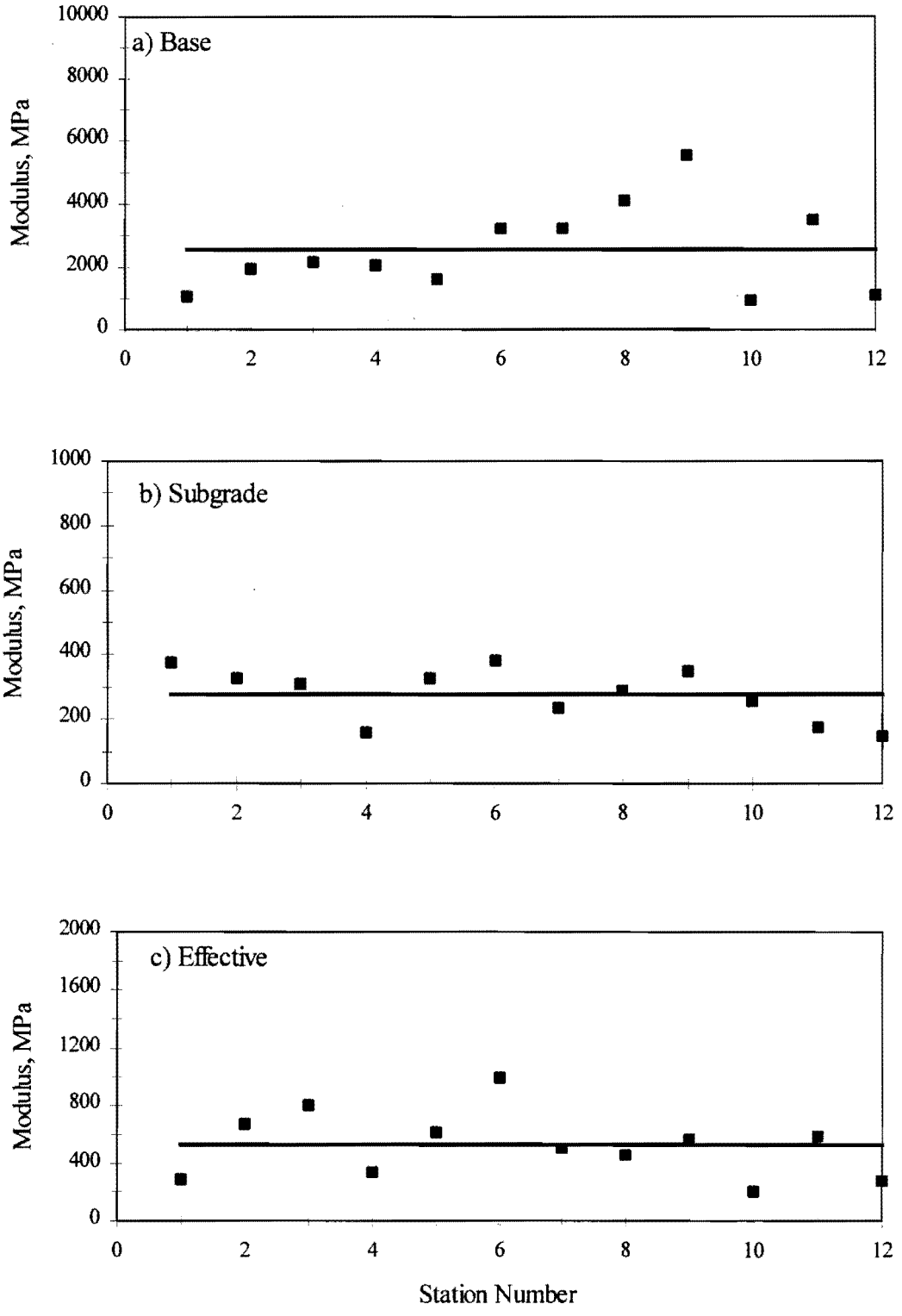

Figure A4 - Results from SPA Tests at FM2446

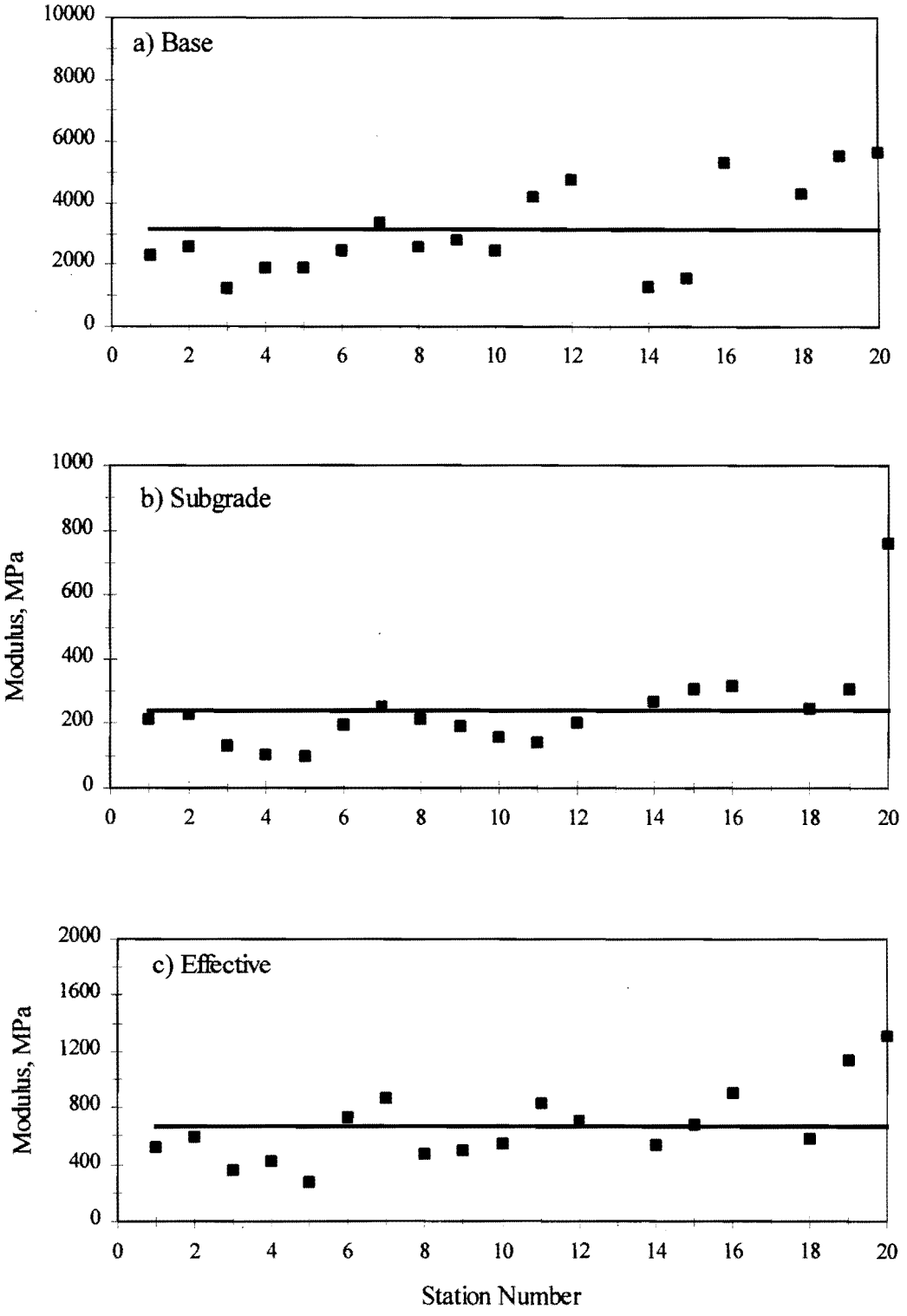

Figure A5 - Results from SPA Tests at FM 1995

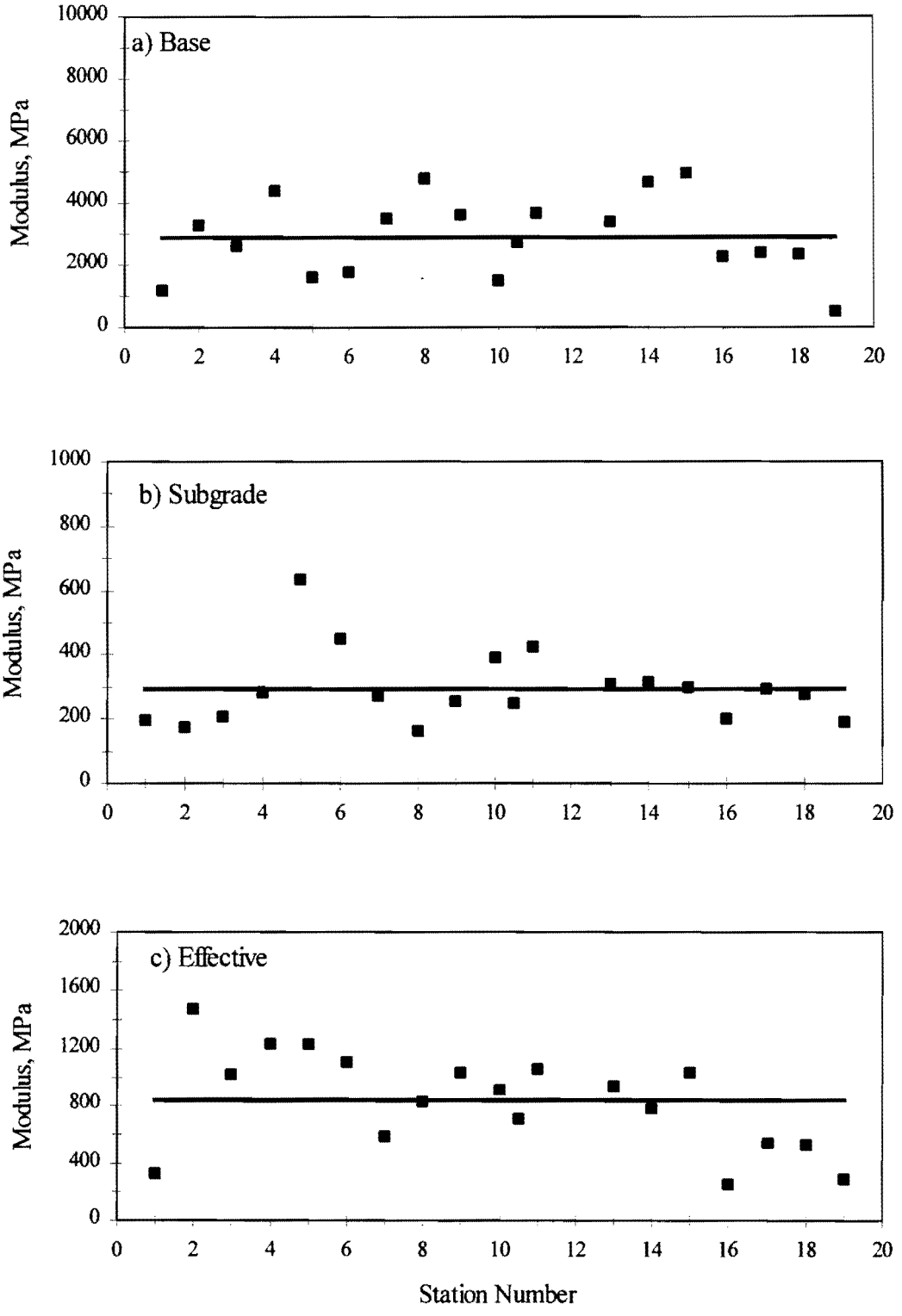

Figure A6 - Results from SPA Tests at FM 1124

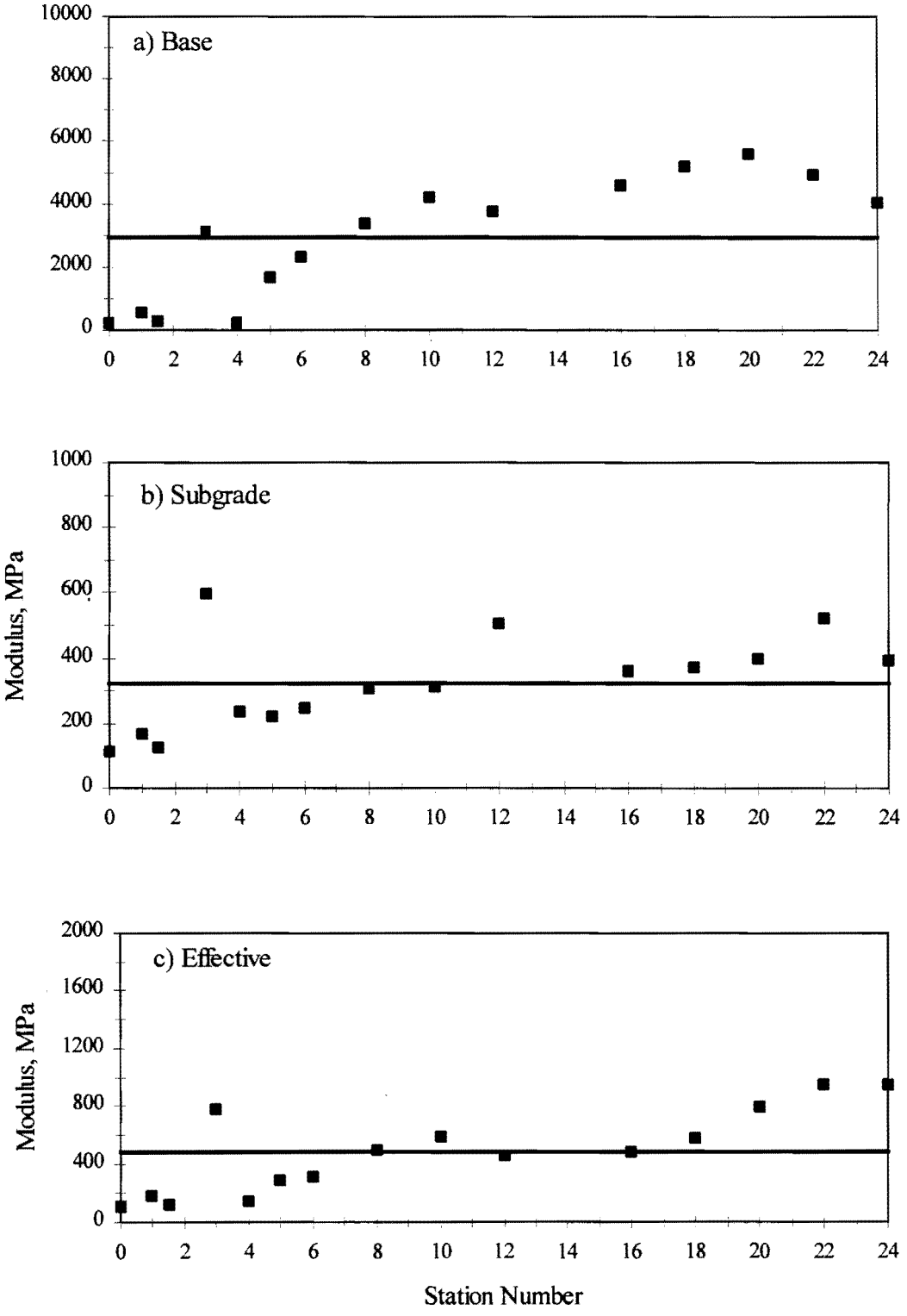

Figure A7 - Results from SPA Tests at FM2446